J. Membrane Biol. 37, 99–136 (1977)

Anion Transport Across the Red Blood Cell Membrane Mediated by Dielectric Pores

K.F. Schnell

Institut für Physiologie, Universität Regensburg, P.O. Box 397, D-8400 Regensburg, Germany

Received 9 November 1976; revised 11 April 1977

Summary. The anion transport across the red blood cell membrane is assumed to occur by ionic diffusion through dielectric pores which are formed by protein molecules spanning the red blood cell membrane. The access of anions to the dielectric pores is regulated by anion adsorption sites positioned at the entrances of the pores. The adsorption of small inorganic anions to the adsorption sites is facilitated by ionizing cationic groups setting up a surface potential at the respective membrane surfaces. Applying the transition state theory of rate processes, flux equations for the unidirectional flux were derived expressing the unidirectional flux as a function of the fractional occupancies of anion adsorption sites at both membrane surfaces.

The basic properties of the transport model were investigated. The concentration-dependence and the pH-dependence of the unidirectional fluxes were shown to depend upon the surface charge density and upon the affinity of the transported anion species to the anion binding sites. The concentration-response and the pH-response of the unidirectional fluxes of different anion species may differ substantially even if the anion species are transported by the same anion transport system. The model predicts a characteristic behavior of the Lineweaver-Burk plot and of the Dixon plot.

A comparison between computer simulated and experimentally determined flux curves was made. By choosing a suitable set of parameters, the anion transport model is capable of simulating the concentration-dependencies and the pH-dependencies of the unidirectional sulfate and chloride flux. It is sufficient to change one single constant in order to convert the "sulfate transport system" into a "chloride transport system". Furthermore, the model is capable of predicting the inhibitory action of chloride on the sulfate transport system. No attempts were made to fit the experimental data to the model. The behavior of the model was qualitatively in accordance with the experimental results.

The kinetics of the anion transport across the red blood cell membrane displays a number of features which are indicative of a specific transport system. The anion permeability of the erythrocyte membrane is many orders of magnitude higher than the anion permeability of an

unmodified black lipid membrane. The unidirectional fluxes of chloride [8, 9, 28, 71], iodide [73], sulfate [29, 55, 57] and phosphate (*unpublished results*) saturate, exhibit a characteristic pH-dependence [9, 12, 14, 28, 53, 57, 71, 73] and can be inhibited by a large number of different inhibitors [11–15, 20, 21, 27, 30, 47, 53]. Therefore, it was suggested that the anion transport across the erythrocyte membrane is mediated by a mobile anion carrier [25, 26, 70]. According to the carrier hypothesis, the carrier molecule complexes with the transported anion at the membrane surfaces, forming an electrically neutral anion-carrier complex. Subsequently, the anion-carrier complex is translocated and the anion is released at the opposite membrane surface.

As far as the carrier hypothesis has been explicitly formulated, a symmetric carrier system has been used for the description of the experimental results [8, 9, 25, 26]. The carrier hypothesis covers a great many of the experimental results, but there are some observations which seem to be in contradiction to a simple carrier transport mechanism. Usually a carrier is defined as a membrane constituent which is alternately in contact with the inner or the outer membrane surface [42]. Consequently, it should be possible to inhibit a carrier system from either membrane side. Previous studies with red blood cell ghosts, however, have shown that the inhibition of the sulfate and the chloride exchange is highly asymmetric. Some nonpenetrating inhibitors, such as phlorizin [39, 56] and DAS (4,4′-diacetamidostilbene-2,2′-disulfonic acid) [34, 74], which cause a strong inhibition of the anion exchange if acting on the outer membrane surface were found to be completely ineffective if acting on the inner membrane surface. In contrast, the sugar transport system can be inhibited by phlorizin [39, 56] and phloretin [2] from the outer and from the inner membrane surface equally well.

Moreover the classical concept of a mobile carrier moving together with the substrate across the membrane is difficult to reconcile with modern concepts of the membrane ultrastructure. Recent biochemical studies have shown that a membrane protein with a molecular weight of 95,000 daltons (95 K) plays a decisive role in anion transport across the red blood cell membrane [5–7, 37, 46, 74]. The 95-K membrane protein can be isolated and enhances the sulfate permeability of lecithin vesicles [51]. The 95-K protein spans the membrane and seems to be in contact with the inner and the outer membrane surface [43, 60, 61]. If a ligand of the 95-K protein would serve as a mobile carrier, the transport of anions should be associated with a displacement of this ligand over the whole membrane thickness. A displacement of a ligand of a protein molecule

over a distance of about 50 Å seems to be extremely unlikely under physiological conditions. On the other hand, the 95-K protein could easily form an anion permeable channel which traverses the red cell membrane and which is responsible for the anion transport.

In this paper, the anion transport across the red blood cell membrane is assumed to occur by ionic diffusion through localized membrane domains. These membrane domains are designated as dielectric pores. The access of small inorganic anions to the dielectric pores is assumed to be regulated by anion adsorption sites positioned on the inner and the outer membrane surface. The fraction of occupied sites on the membrane surface, in turn, is assumed to be modified by ionizing cationic fixed charges which set up a surface potential and thereby facilitate the adsorption of anions to the anion binding sites. On the basis of these assumptions, a model for the anion transport across the red blood cell membrane has been developed. The basic properties of the transport model were investigated and compared to the experimental results. According to the anion transport model, the concentration-response and the pH-response of the unidirectional anion flux is strongly dependent upon the surface charge density and upon the affinity of the transported anion species to the anion adsorption sites at the membrane surfaces. Thus entirely different concentration-dependencies and pH-dependencies of the unidirectional fluxes of two anion species may be observed, even if both anion species are transported by the same anion transport system. In addition, the inhibitory action of a second anion species on the unidirectional flux of the first anion species was studied. The model predicts a characteristic pattern of concentration-dependence of the unidirectional fluxes. The computer-simulated Lineweaver-Burk plots and Dixon plots display particular features which have been previously observed in studies on the chloride [10] and on the sulfate transport [57] in human erythrocytes. Making suitable assumptions of the surface charge density and on the affinity of the transported anion to the anion adsorption sites, the model is capable of simulating the experimentally observed concentration-dependence and pH-dependence of the unidirectional fluxes of sulfate and chloride and of predicting the action of cloride on the unidirectional sulfate flux.

Materials and Methods

The experiments were performed with blood from healthy adult donors. The blood was withdrawn under sterile conditions and stored maximally for 6 days at 4 °C.

Coagulation was prevented by adding an acid-citrate-dextrose solution. Before the experiments, the red blood cells were washed three times in a 165 mM NaCl solution; plasma and buffy coat were removed. For chloride depletion, 4 g tightly packed red cells (10 min centrifugation at $5000 \times g$, 20 °C, pH 7.3) were incubated three times for about 15 min in 10 volumes of a 132 mM K_2SO_4 solution (37 °C, pH 7.2). Then the cells were incubated in 36 ml of a solution containing 25 mM K-phosphate buffer, 60 mM sucrose, 5 μg/ml amphotericin B, and variable amounts of K_2SO_4. If the sulfate concentration had to be lowered below 75 mM, we started with a solution containing 75 mM K_2SO_4, 25 mM K-phosphate buffer, and 60 mM sucrose, and then the sulfate concentration was titrated down to the required value by slowly adding a phosphate buffer/sucrose solution (25 mM K-phosphate, 60 mM sucrose). Simultaneously, pH was adjusted by adding either 0.1 N H_2SO_4 or 0.1 N KOH. The titration procedure usually took 90 min at 37 °C. Finally, the cells were spun down and resuspended in an incubation solution of proper composition and labeled with $^{35}SO_4$.

The labelling of the cells took 45 min at 37 °C and was extended to 120 min at alkaline pH. Thereafter, the cells were transferred into a nonradioactive solution of the same composition, and the tracer efflux from the cells was measured. The sulfate flux measurements were performed with a 10% (w/v) cell suspension. The rate constant k of the sulfate back-exchange was determined by fitting the cpm/time curves to Eq. (1) by means of a least squares fit procedure. The amount of intracellular sulfate n_{in} was calculated from the intracellular radioactivity and the specific activity of sulfate in the incubation solution at isotopic equilibrium.

The tracer back-exchange at Donnan equilibrium follows an exponential equation which at low cell concentrations can be expressed by:

$$y = \bar{y} - (\bar{y} - y_0) \cdot \exp(-k\,t). \tag{1}$$

y (cpm/ml) is the radioactivity in the outside solution at time t, $\bar{y}$ (cpm/ml) and y_0 (cpm/ml) are the total radioactivity per ml suspension and the radioactivity at time zero, k (min^{-1}) is the rate constant for the tracer back-exchange and t (min) is time. The unidirectional flux $\vec{J}$ is given by:

$$\vec{J} = k \cdot n_{in}. \tag{2}$$

n_{in} is the amount of intracellular sulfate per g cells wet weight. The wet weight of the cells was determined prior to any other manipulations under standardized conditions (10 min centrifugation at $5000 \times g$, pH 7.3, 20 °C). 1 g cells wet wt corresponds to a dry wt of 0.353 ± 0.003 g (n = 141, average ±SD). Thus the unidirectional sulfate fluxes can be expressed in moles · min^{-1} · g cells dry wt^{-1}.

The unidirectional chloride fluxes were supplied by Dalmark. For technical details the reader is referred to Dalmark [9]. The chloride fluxes are expressed in moles · min^{-1} · 3×10^{13} $cells^{-1}$. Since 1 g cells dry wt under the above conditions contains 3.0×10^{10} cells, the sulfate fluxes can be expressed in the same units as the chloride fluxes by multiplying the sulfate fluxes with a factor of 1000. It should be noted however, that the chloride and the sulfate flux measurements were conducted at different temperatures and therefore are not strictly comparable.

Results

Outline of the Model

In this paper the erythrocyte membrane is considered to be composed of a lipid bilayer into which large protein molecules are inserted. The

lipid molecules are oriented with their polar head groups towards the water phases whereas the hydrophobic chains of the lipidic acids are positioned inside the membrane. The protein molecules with their hydrophobic moieties are in close contact with the lipid bilayer. The polar groups of the protein molecules are mainly located at the outer and at the inner membrane surfaces.

According to the transition state theory [16, 22, 33], the elementary process in diffusion is the jumping of an ion over a potential barrier separating two potential minima. In order to scale barrier, the ion has to possess a certain minimum energy which will, in general, substantially exceed the average thermal energy of the ions. The diffusion resistance of a localized membrane region is determined by the height of the energy barrier(s) which the ion has to overcome in order to penetrate the membrane. The height of the main diffusion barrier of the cellular membrane is assumed to be approximately equal to the dielectric energy of the ion within the membrane which, according to the Born equation [3], is determined by the dielectric constant of the water phase and by the dielectric constant of the respective membrane domain. Since the bulk material of the lipid bilayer regions is composed of the hydrocarbon chains of the lipidic acids, the dielectric constant of the bilayer regions of the cell membranes is supposed to be much smaller than the dielectric constant of the protein regions. Thus, the diffusion resistance of the lipid regions of the cell membrane for ions should be much higher than the diffusion resistance of the protein regions. It was therefore suggested that the membrane proteins could act as dielectric pores which facilitate the transport of ions across the cell membrane [44, 67].

For the derivation of an anion transport model, a number of important experimental results have to be taken into account: (i) As already mentioned, the anion transport across the erythrocyte membrane is mediated by a specific membrane protein [5–7, 37, 46, 74] which penetrates the red blood cell membrane and seems to be in contact with both membrane surfaces [43, 60, 61]. This protein presumably acts as a dielectric pore providing a penetration route for anions across the red blood cell membrane. (ii) The unidirectional fluxes of chloride [8, 9, 28, 72], iodide [73], and sulfate [57], which have been most intensively studied, exhibit a saturation kinetics. The saturation of the fluxes indicates that the anions on their way across the erythrocyte membrane interact with a limited number of membrane sites. These sites are supposed to be located on the membrane surfaces at the entrance of the dielectric pores and are supposed to regulate the access of anions to the

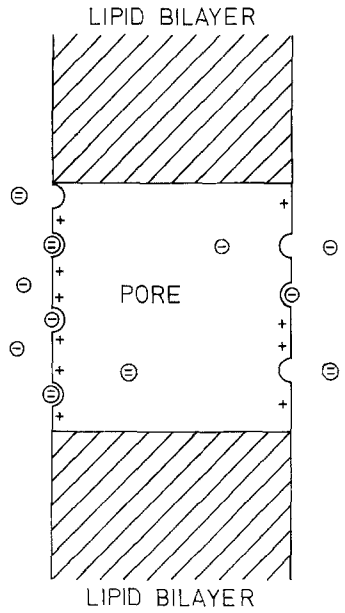

Fig. 1. Schematic representation of the membrane model. The bilayer region of the cellular membrane is interrupted by a pore which is built by a membrane protein traversing the red blood cell membrane

dielectric pores. Furthermore, a competition between the various anion species is observed [10, 57] suggesting that small inorganic anions are transported by the same anion transport system. (iii) Finally, the anion transport across the red blood cell membrane is inhibited by various amino group reagents [5–7, 35, 37, 45, 50, 74], whereas sulfhydryl group reagents were found to be completely ineffective in inhibiting anion transport [35, 62]. These results give strong evidence towards the assumption that amino groups are directly involved in the regulation of the anion permeability by facilitating the adsorption of small inorganic anions to the anion adsorption sites on the membrane surfaces [45, 47].

A schematic representation of the membrane model used for the description of anion transport across the erythrocyte membrane is shown in Fig. 1. The equations for the unidirectional fluxes derived in the subsequent sections are based upon the following assumptions: (i) The anion transport across the red blood cell membrane occurs by ionic diffusion through dielectric pores. (ii) The access of anions to the dielectric pores is regulated by anion adsorption sites at the inner and the outer entrance of the pores. Each binding site binds a single monovalent or divalent anion. (iii) The fraction of occupied sites is modified by the

surface potentials which are supposed to be set up by ionizing cationic groups at the inner and the outer membrane surface.

For the description of the diffusion process, the formalism of the transition state theory was applied. To express the unidirectional fluxes in terms of the free energy profile of a multibarrier membrane is a complicated matter, particularly if interactions amongst the penetrating ions have to be taken into consideration. In such an event, the energy profile of the membrane is modified in a manner depending upon the concentration distribution of ions within the membrane. We made no attempts to solve the problem for a multibarrier membrane, rather we proceeded at once to a situation where one of the energy barriers is much higher than the others. The transport of anions across the high diffusion barrier will then be the rate-determining step for the anion transport and the ions to the left and to the right of the high diffusion barrier may be assumed to have attained their equilibrium distribution.

Fig. 2 exhibits the hypothetical energy profile of a dielectric pore. The two outer barriers represent the interfacial barriers at the outer and the inner membrane surfaces. The intermediate barrier represents the main diffusion barrier of the erythrocyte membrane for small inorganic anions, which is assumed to consist of a more hydrophobic portion of the membrane protein molecule. The energy minima at the inner and the outer membrane surfaces refer to the energetic state of the anions adsorbed to the anion binding sites. It should be emphasized that in general, the energy profiles for different anion species are different even if they morphologically use the same penetration route across the erythrocyte membrane.

In the subsequent section we first calculate the surface concentrations of contact-adsorbed anions bound to the adsorption sites. Then the unidirectional flux can be expressed as a function of the concentration of contact-absorbed anions at the outer and the inner membrane surfaces.

The Surface Concentration of Contact-Absorbed Anions

In order to calculate the surface concentrations of contact-adsorbed anions at the membrane surfaces, the surface potential and the number of adsorption sites within this particular membrane area have to be known. As delineated above, we assume that the surface potential is set up by ionizing cationic groups which are clustered at the entrances of the

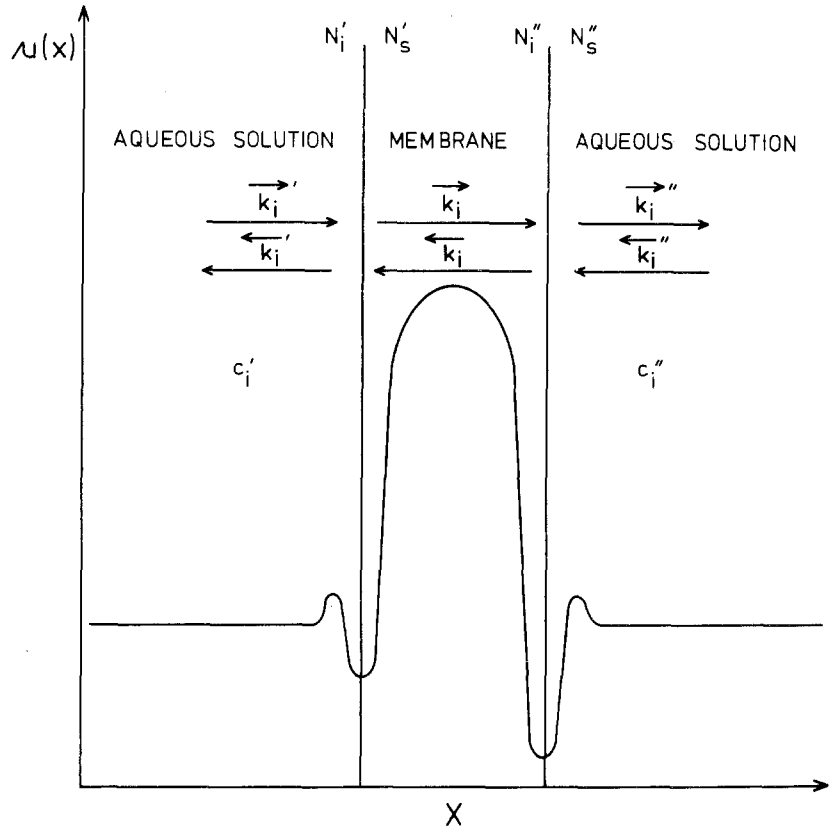

Fig. 2. Energy profile of a dielectric pore

dielectric pores. The surface charge density σ_s (amp $\times$ sec $\times$ cm^{-2}) is then given by:

$$\sigma_s = \sigma_{\max} \frac{H \exp(-\varphi_0)}{K + H \exp(-\varphi_0)}. \tag{3}$$

$\sigma_{\max}$ (amp $\times$ sec $\times$ cm^{-2}) is the maximal electrical charge per unit area if all cationic groups are protonated, H (cm^{-3}) is the proton concentration in the adjacent aqueous phase, K (cm^{-3}) is the ionization constant of the cationic groups and $\varphi_0 = q\psi_0/kT$ is a reduced surface potential (ψ_0 is the surface potential (V), q the electrical elementary charge, k the Boltzman constant and T the absolute temperature). The term $H \exp(-\varphi_0)$ in Eq. (1) denotes the surface concentration of protons.

The relation between the surface charge density σ_s and the surface potential φ_0 at a planar solid/electrolyte solution interface is given by the

Gouy-Chapman theory of the electrical double layer [23]:

$$\sigma_s = \sqrt{2\varepsilon\varepsilon_0 k\,\mathrm{T}\sum_{i=1}^{n} c_i\{\exp(-z_i\varphi_0)-1\}}\,. \tag{4}$$

Here ε and ε_0 are the dielectric constants for water and the permitivity of free space, c_i (cm^{-3}) is the concentration and z_i the valency of the i-th ion species, respectively.

Combining Eqs. (3) and (4) yields Eq. (5) which expresses the surface potential φ_0 as a function of the membrane parameters $\sigma_{\max}$ and K and as a function of the electrolyte composition and of pH of the adjacent aqueous phase.

$$\sigma_{\max}\frac{H\cdot\exp(-\varphi_0)}{K+H\cdot\exp(-\varphi_0)} = \sqrt{2\varepsilon\varepsilon_0 k\,\mathrm{T}\sum_{i=1}^{n} c_i\{\exp(-z_i\varphi_0)-1\}}\,. \tag{5}$$

It should be noted that in Eqs. (3)–(5), the concentrations are expressed in number of particles per cm^3. If the concentrations are expressed in moles/liter, they have to be converted to the appropriate dimension. Inserting $\sigma_{\max}$ and K, the surface potential φ_0 is obtained by solving Eq. (5) numerically.

Assuming suitable values of $\sigma_{\max}$ and K for the left and the right membrane surface, the surface potentials can be calculated by means of Eq. (5). Knowing the surface potentials and assuming equilibrium at the membrane surfaces, the surface concentrations N_i of contact-adsorbed anions of the ith anion species are obtained by Eqs. (6) and (7) which can be readily derived on the basis of kinetic considerations (for notation compare Fig. 2):

$$N_i' = N_s' \frac{c_i'\exp(-z_i\varphi_0')}{K_{si}'\left(1+\sum\limits_{\substack{j=1\\ j\neq i}}^{n} c_j'\exp(-z_j\varphi_0')/K_{sj}'\right)+c_i'\exp(-z_i\varphi_0')} \tag{6}$$

$$N_i'' = N_s'' \frac{c_i''\exp(-z_i\varphi_0'')}{K_{si}''\left(1+\sum\limits_{\substack{j=1\\ j\neq i}}^{n} c_j''\exp(-z_j\varphi_0'')/K_{sj}''\right)+c_i''\exp(-z_i\varphi_0'')} \tag{7}$$

N_s is the maximal surface concentration of anions at the respective membrane surface which is determined by the number of available anion adsorption sites. c_i and c_j are the concentrations of the ith and the jth anion in the water phase, z_i and z_j are the valencies of the ith and the jth

anion, and K_{si} and K_{sj} are the dissociation constants for the site-anion complexes for the ith and the jth anion species, respectively. The terms $c_i \cdot \exp(-z_i\varphi_0)$ and $c_j \cdot \exp(-z_j\varphi_0)$ in Eqs. (6) and (7) denote the surface concentration of mobile anions of the ith and the jth species at the membrane surface.

The dissociation constants K_{si} and K_{sj} are defined for the left and for the right membrane surface as follows:

$$K'_{si} = \vec{k}'_{i0} N'_s / \overleftarrow{k}'_{i0} \tag{8}$$

$$K'_{sj} = \vec{k}'_{j0} N'_s / \overleftarrow{k}'_{j0} \tag{9}$$

$$K''_{si} = \vec{k}''_{i0} N''_s / \overleftarrow{k}''_{i0} \tag{10}$$

$$K''_{sj} = \vec{k}''_{j0} N''_s / \overleftarrow{k}''_{j0} \tag{11}$$

k_{i0} and k_{j0} are the rate constants for the flux of the ith and the jth anion across the left (index′) and the right (index″) interfacial barrier if the surface potential is equal to zero. The arrows above the rate constants indicate the direction of the reaction (Fig. 2).

The Transport of Anion across the Main Diffusion Barrier

As already pointed out, the elementary process in diffusion is the jumping of an ion across a potential barrier. The rate constant for the diffusive jump is determined by the free energy of activation, i.e., by the energy required for the ion to pass from its current equilibrium position to the top of the energy barrier [16, 22, 33]. The free energy of activation is modified by the electrical potential $\Delta\psi$ which acts across the respective energy barrier. Assuming that the potential barrier lies half way between two neighboring potential minima and assuming that the potential drops linearly over the barrier, the change of the free energy of activation due to the electrical potential is $z_i q \Delta\psi/2$ for the diffusive jump in the forward direction and $-z_i q \Delta\psi/2$ for the diffusive jump in the reverse direction [75]. By introducing again a reduced electrical potential $\Delta\varphi = q\Delta\psi/kT$, the rate constant $\vec{k}_i$ and $\overleftarrow{k}_i$ for the diffusive jump in either forward or the reverse direction can be written as

$$\vec{k}_i = \vec{k}_{i0} \exp(z_i \Delta\varphi/2) \tag{12}$$

$$\overleftarrow{k}_i = \overleftarrow{k}_{i0} \exp(-z_i \Delta\varphi/2) \tag{13}$$

with $\vec{k}_{i0}$ and $\overleftarrow{k}_{i0}$ being the respective rate constants if $\Delta\varphi$ is zero.

In addition, a limited number of anion adsorption sites was assumed at each membrane surface which regulates the access of anions to the dielectric pores. The probability that an anion jumps across the membrane is proportional to the concentration of contact-adsorbed anions at the *cis*-membrane side times the probability of finding an empty site at the *trans*-membrane side. Thus the unidirectional flux $\vec{J}_i$ of the ith anion from the left to the right is given by:

$$\vec{J}_i = \vec{k}_{i0} \exp(z_i \Delta\varphi/2)\, N_i' \left(1 - \sum_{i=1}^{n} N_i''/N_s''\right). \tag{14}$$

Correspondingly, the unidirectional flux $\overleftarrow{J}_i$ from the right to the left is given by:

$$\overleftarrow{J}_i = \overleftarrow{k}_{i0} \exp(-z_i \Delta\varphi/2)\, N_i'' \left(1 - \sum_{i=1}^{n} N_i'/N_s'\right). \tag{15}$$

Again N_i' and N_i'' denote the surface concentrations of the ith anion; N_s' and N_s'' denote the maximal suface concentration of anions at the left (index′) and at the right (index″) membrane surfaces, respectively. The terms

$$\left(1 - \sum_{i=1}^{n} N_i'/N_s'\right) \quad \text{and} \quad \left(1 - \sum_{i=1}^{n} N_i''/N_s''\right)$$

in Eqs. (14) and (15) express the probabilities of finding a vacant site at the opposite membrane surface.

The netflux J_i of the ith anion species is the sum of the two opposingly directed unidirectional fluxes $\vec{J}_i$ and $\overleftarrow{J}_i$, where the unidirectional flux $\overleftarrow{J}_i$ from the right to the left has to be considered mathematically as the negative flux:

$$J_i = \vec{J}_i - \overleftarrow{J}_i. \tag{16}$$

Since the unidirectional anion fluxes were measured at equilibrium, the net flux is equal to zero. Making use of the equilibrium condition, the electrical potential is obtained by the following expression:

$$\Delta\varphi = \frac{1}{z_i} \ln \frac{\overleftarrow{k}_{i0} N_i'' \left(1 - \sum_{i=1}^{n} N_i'/N_s'\right)}{\vec{k}_{i0} N_i' \left(1 - \sum_{i=1}^{n} N_i''/N_s''\right)}. \tag{17}$$

Substituting Eq. (17) into (14) yields the following:

$$\vec{J}_i = \sqrt{\vec{k}_{i0}\overleftarrow{k}_{i0}\, N_i' \left(1 - \sum_{i=1}^{n} N_i''/N_s''\right) N_i'' \left(1 - \sum_{i=1}^{n} N_i'/N_s'\right)} \tag{18}$$

which expresses the unidirectional anion flux as a function of the concentration of contact-adsorbed anions at both membrane surfaces and of the rate constants for the forward and the reverse reactions. For experimental purposes, it may be more convenient to express the unidirectional flux as a function of the fraction of occupied sites N_i/N_s. Eq. (18), therefore, may be rewritten as:

$$\vec{J}_i = \vec{J}_{\max(i)} \sqrt{(N_i'/N_s')\left(1 - \sum_{i=1}^{n} N_i''/N_s''\right)(N_i''/N_s'')\left(1 - \sum_{i=1}^{n} N_i'/N_s'\right)} \tag{19}$$

with

$$\vec{J}_{\max(i)} = \sqrt{\vec{k}_{i0} N_s' \overleftarrow{k}_{i0} N_s'}. \tag{20}$$

Basic Features of the Model

In the preceding section, the unidirectional flux $\vec{J}_i$ of the ith anion was shown to be a function of the concentrations of contact-adsorbed anions N_i' and N_i'' of the ith anion species at both membrane surfaces. The concentrations of contact-adsorbed anions in turn, are complicated functions of the concentrations of the ith anion, of pH and of the electrolyte composition of the aqueous solution adjacent to the respective membrane surface. In order to study the basic features of the anion transport model the following simplifying assumptions were made: (i) We restrict our considerations to a single electrolyte, where only the anion species 1 is present. (ii) The membrane is symmetric. (iii) The electrolyte composition and pH of the solution at both membrane sides are identical. Under these conditions the indices $'$ and $''$ can be omitted. Eqs. (6) and (7) then reduce to:

$$N_1 = N_s \frac{c_1 \exp(-z_1 \varphi_0)}{K_{s1} + c_1 \exp(-z_1 \varphi_0)} \tag{21}$$

and the unidirectional flux $\vec{J}_1$ of the anion species 1 is given by:

$$\vec{J}_1 = \vec{J}_{\max(1)}(N_1/N_s)(1 - N_1/N_s). \tag{22}$$

The symbols have the meaning as defined in the preceding sections.

Eq. (21) describes the adsorption of the anion species 1 to an electrically charged surface with a limited number of adsorption sites. The fractional occupancy of the sites at a given anion concentration is determined by the free energy of adsorption which arbitrarily may be subdivided into a "chemical energy term" and into an "electrostatic energy term". The dissociation constant K_{s1} is determined by the chemical energy of adsorption which under our conditions is supposed to be constant and to be a function of the chemical properties of the transport anion species. On the other hand, the electrostatic energy term $z_1\varphi_0$ is variable. The electrical energy term is a function of the surface potential φ_0 and of the electrical charge of the transported anion, but it is independent of chemical properties of the transported anion species.

The examination of Eq. (21) is shown in Fig. 3. The fraction of occupied sites N_1/N_s is plotted *vs.* the anion concentration c_1 and *vs.* pH. σ_{max} and K_{s1} are indicated in the figure. There are two results which are of particular interest. Firstly, the adsorption isotherms differ substantially from a Langmuir adsorption isotherm. If the surface charge density σ_{max} is high and if pH is much smaller than the pK of the charge determining cationic groups at the membrane surface, the apparent half-saturation constant is much higher than the dissociation constants K_{s1} used for the computation of the curves. Furthermore, the fraction of occupied sites under these conditions becomes rather insensitive against variations of the bulk concentration c_1 and is mainly determined by the surface charge density. This can result in an abrupt increase of the adsorption isotherms so that the curves do not seem to start at point zero. Secondly, if both the fixed charge density σ_{max} and the dissociation constant K_{s1} are high, the fraction of occupied sites is strongly pH-dependent. On the other hand, if K_{s1} is small, i.e., if the chemical adsorption forces become predominant, the fractional occupancy of the anion adsorption sites becomes invariable against changes in pH.

The inspection of Eq. (22) shows that within the range of $0<N_1/N_s<0.5$ the unidirectional flux $\vec{J}_1$ increases as the fraction of occupied sites is raised, reaching a maximum at $N_1/N_s=0.5$ when the membrane surfaces are half-saturated. Above $N_1/N_s=0.5$, a blocking effect becomes predominant at a further increase of the fractional occupancy and the fluxes fall off again.

As shown in Fig. 4, the unidirectional fluxes display a complex pattern of concentration-responsiveness and pH-responsiveness. Depending upon the choice of σ_{max} and K_{s1}, the flux curves either increase or decrease within a distinct concentration range or they may exhibit a

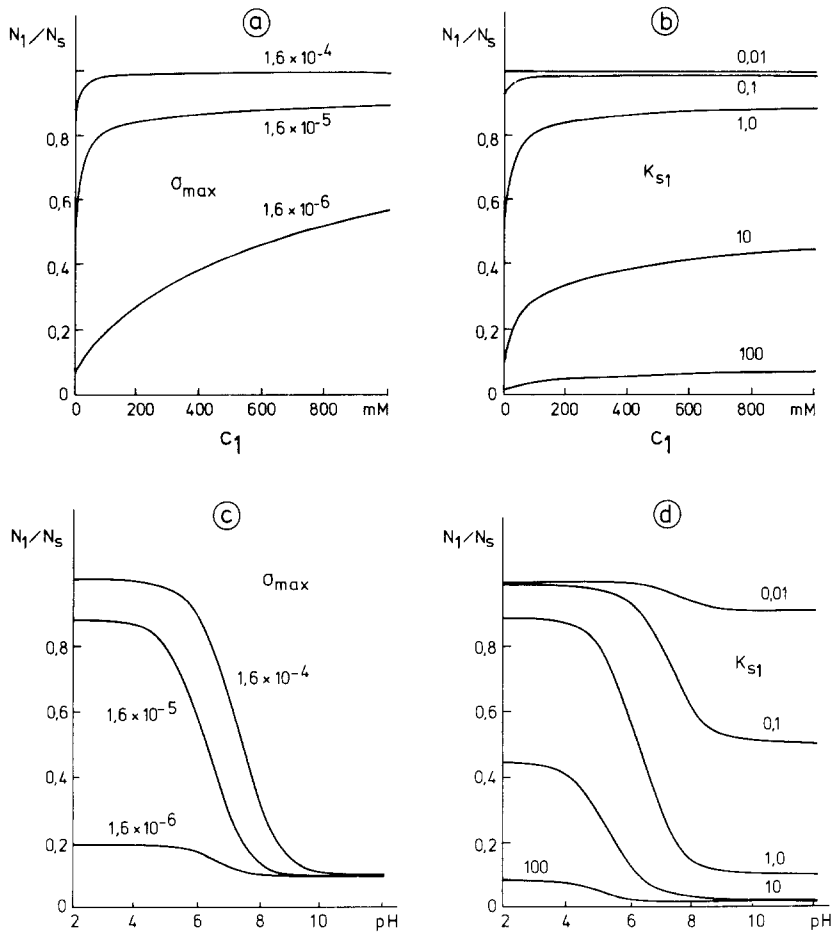

Fig. 3. Adsorption of anions to a positively charged membrane surface carrying a limited number of anion adsorption sites. (*a*) Effects of the surface charge density σ_{max} and (*b*) of the site-anion dissociation constant K_{s1} upon the surface concentration of adsorbed anions. The fraction of occupied sites N_1/N_s is plotted *vs.* the anion concentration c_1 mM; pH = 5.0. (*c*) Effect of the surface charge density σ_{max} and (*d*) of the site-anion dissociation constant K_{s1} upon concentration of adsorbed anions. The fraction of occupied sites N_1/N_s is plotted as a function of pH; $c_1 = 0.1$ M. The calculations were performed for a single monovalent electrolyte such as KCl by using Eqs. (5) and (21). Parameters used for the calculation: σ_{max} (amp·sec·cm^{-2}) and K_{s1}(M) as indicated in the figures. $K = 1 \times 10^{-7}$ M. (*a*) $K_{s1} = 1$ M; (*b*) $\sigma_{max} = 1.6 \times 10^{-5}$ amp·sec·cm^{-2}; (*c*) $K_{s1} = 1$ M; (*d*) $\sigma_{max} = 1.6 \times 10^{-5}$ amp·sec·cm^{-2}

concentration maximum. Correspondingly, the pH-profile of the flux curves is strongly affected by variations of σ_{max} and K_{s1}. Figs. 4*c* and *d* demonstrate that, depending upon the choice of σ_{max} and K_{s1}, entirely different types of pH-dependencies of the flux curves were observed. The

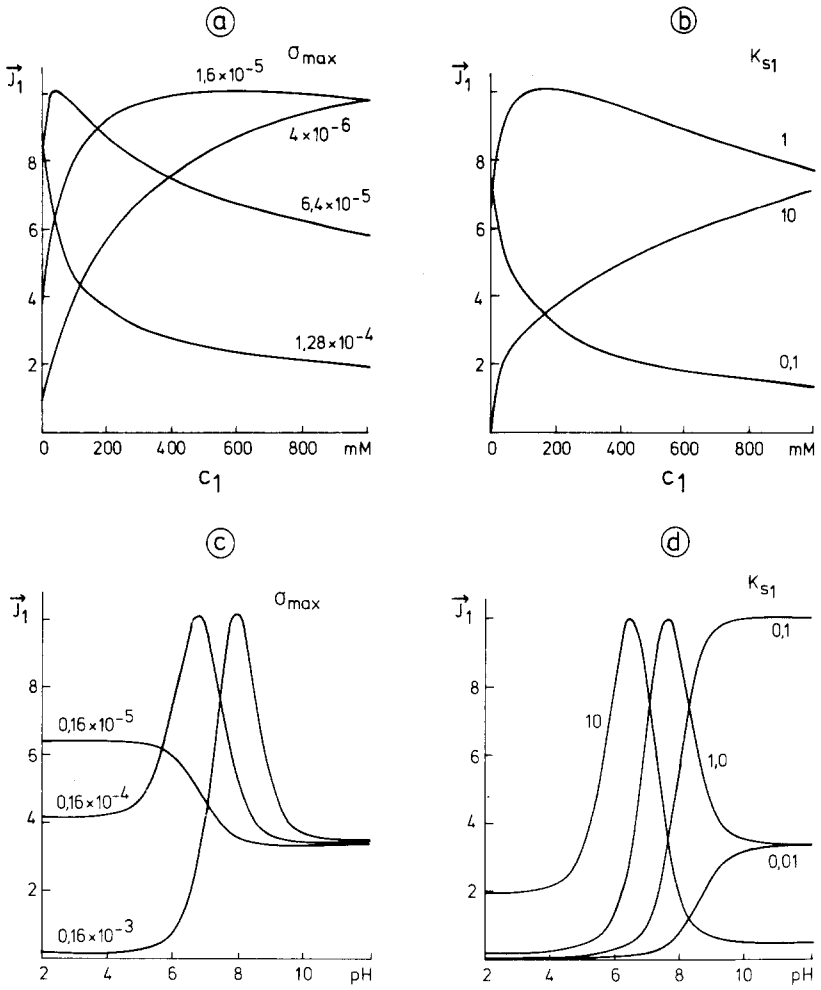

Fig. 4. Concentration-dependence and pH-dependence of the unidirectional anion flux across a symmetric membrane. (*a*) Effect of the surface charge density σ_{max} and (*b*) of the site-anion dissociation constant K_{s1} on the unidirectional anion flux. The unidirectional flux $\vec{J}_1$ (arbitrary units) is plotted as a function of the anion concentration c_1(mM); pH = 7.0. (*c*) Effect of the surface charge density σ_{max} and (*d*) of the site-anion dissociation constant K_{s1} upon the pH-dependence of the unidirectional flux. $c_1 = 100$ mM. The flux $\vec{J}_1$ (arbitrary units) is plotted *vs.* pH. Parameters used for the calculation: (*a*) $K_{s1} = 2$ M; (*b*) $\sigma_{max} = 1.6 \times 10^{-5}$ amp · sec · cm^{-2}; (*c*) $K_{s1} = 1$ M; (*d*) $\sigma_{max} = 1.6 \times 10^{-4}$ amp · sec · cm^{-2}. The maximal surface charge density σ_{max}(amp · sec · cm^{-2}) and the site-anion dissociation constant K_{s1} (M) are indicated in the figures. The ionization constants K' for the left and K'' for the right membrane surface were set to 1×10^{-7}(M). The calculations were performed for a single divalent electrolyte such as K_2SO_4 by using Eqs. (5), (21) and (22)

fluxes either increase or decrease with increasing pH, or they show pH-maxima at different locations.

For a symmetric membrane, if two anion species are present, the

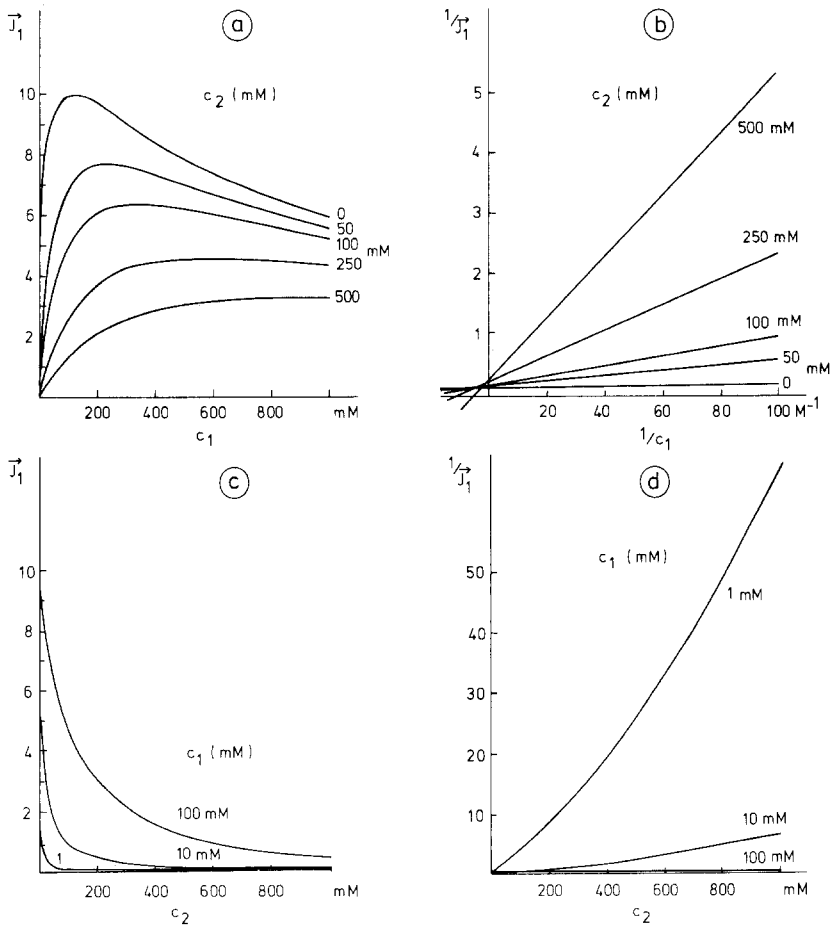

Fig. 5. The action of anion species 2 upon the unidirectional flux of anion species 1. (*a*): Concentration-dependence of the unidirectional flux $\vec{J}_1$ (arbitrary units) in the presence of various concentrations of the anion species 2. The flux $\vec{J}_1$ (arbitrary units) is plotted *vs.* the concentration c_1 (mM) of the 1st anion species. The concentration c_2 (mM) of the anion species 2 is indicated at the respective curves. (*b*): Lineweaver-Burk plot made from the ascending branches of the flux/concentration curves shown in *a*. The ascending branches of the flux curves were used. (*c*): Dose-response curves. The flux $\vec{J}_1$ (arbitrary units) of the anion species 1 is plotted *vs.* the concentration c_2 (mM) of the anion species 2. The concentration c_1 (mM) of the anion species 1 is indicated at the respective curves. (*d*): Dixon plots made from the dose-response curves shown in *c*. The calculations were performed for two monovalent electrolytes and for a symmetric membrane. For the computation of the curves, Eqs. (5), (23), (24) and (25) were used. Parameters used for the computation $\sigma'_{max} = \sigma''_{max} = 1.6 \times 10^{-5}$ (amp · sec · cm^{-2}); $K' = K'' = 1 \times 10^{-7}$ (M); $K'_{s1} = K''_{s1} = 0.5$ (M); $K'_{s2} = K''_{s2} = 0.5$ (M); $z_1 = -1$; $z_2 = -1$; pH = 7.0

following set of equations has to be used: The surface concentration N_1 of the 1st anion (subscript 1) is:

$$N_1 = N_s \frac{c_1 \exp(-z_1 \varphi_0)}{K_{s1}(1 + c_2 \exp(-z_2 \varphi_0)/K_{s2}) + c_1 \exp(-z_1 \varphi_0)} \tag{23}$$

and the surface concentration N_2 of the second anion species (subscript 2) is given by:

$$N_2 = N_s \frac{c_2 \exp(-z_2\varphi_0)}{K_{s2}(1 + c_1 \exp(-z_1\varphi_0)/K_{s1}) + c_2 \exp(-z_2\varphi_0)}. \quad (24)$$

The unidirectional flux $\vec{J}_1$ of the 1st anion species then is obtained by:

$$\vec{J}_1 = \vec{J}_{\max(1)}(N_1/N_s)\left(1 - \sum_{i=1}^{2} N_i/N_s\right). \quad (25)$$

c_1 and c_2 are the concentrations of the 1st and the 2nd anion within the water phase; K_{s1} and K_{s2} are the dissociation constants of the site-anion complexes.

In order to study the inhibition of the unidirectional flux $\vec{J}_1$ of the 1st anion by a 2nd anion, the following procedures are applied: either the concentration dependence of $\vec{J}_1$ in the presence of different concentrations c_2 of the anion species 2 is studied (Fig. 5*a*) or the effect of increasing concentrations c_2 of the anion species 2 upon $\vec{J}_1$ is studied (Fig. 5*c*).

The concentration response of the flux curves shows some typical features (Fig. 5*a*). $\vec{J}_1$ exhibits a concentration maximum which for increasing c_2 shifts towards higher concentrations of c_1 and finally seems to disappear. The actually observed maximal flux of the anion species 1 is reduced and the apparent half-saturation constant increases as c_2 is raised. This behavior is usually interpreted as an inhibition which is partially competitive and partially noncompetitive. Fig. 5*b* displays a Lineweaver-Burk plot made from the ascending branches of the flux/concentration curves shown in Fig. 5*a*. A linear relation between $1/\vec{J}_1$ and $1/c_1$ is observed, but the straight lines do not intersect at one point. Figs. 5*c* and *d* display dose-response curves for three different concentrations of c_1 and the corresponding Dixon plots. An overlinear increase of $1/\vec{J}_1$ with increasing c_2 was observed. At low c_2, the curves can be approximated by straight lines which distinctly intersect above the abscissa. This behavior can only be seen if Fig. 5*d* is plotted on a larger scale.

The results of our studies are of great theoretical interest. They show that the unidirectional fluxes of two anion species may exhibit a completely different concentration-response and pH-response even if both anion species are transported by the same transport system. As indicated by our studies, the concentration-dependence and the pH-dependence of the unidirectional flux is strongly dependent upon the choice of the surface

charge density and upon the affinity of the transported anion species to the anion binding sites which is expressed by the K_{si}. Furthermore, we have to expect characteristic deviations of the Lineweaver-Burk and the Dixon plots.

Comparison between Experimental and Theoretical Results

A test of the anion transport model would consist of an attempt to simulate the kinetics of the anion transport across the red blood cell membrane. From the various anion species, the transport of sulfate and of chloride across the red cell membrane has been most extensively investigated. It seems interesting, therefore, to study to which extent the above model is capable of giving a description of the sulfate and the chloride transport under the various experimental conditions.

Unfortunately most of the membrane parameters (σ_{max}, K, N_s and $\vec{k}_i$) determining the behavior of the transport model are not known and are not accessible to direct measurement. We therefore tried to find sets of parameters which are suited to simulate the concentration-dependence and the pH-dependence of the unidirectional sulfate and chloride fluxes. Although the parameters were arbitrarily chosen, their choice is subject to some restrictions. Firstly, the parameters have to be of an order of magnitude which is physically reasonable and compatible with our present knowledge of the membrane ultrastructure. Secondly, if sulfate and chloride are both transported by the same transport system, only those parameters can be changed which are determined by the chemical properties of the transported anion species. Hence for the simulation of the sulfate and of the chloride fluxes the same values of σ_{max}, K and N_s have to be used, whereas the K_{si} may be changed.

For the calculation of the unidirectional fluxes Eqs. (5), (6), (7) and (19) were used. The computed fluxes are expressed in arbitrary units. For the calculations, the differences between intracellular and extracellular anion concentrations and between intracellular and extracellular pH arising from the Donnan distribution of ions were ignored. These conditions can only be strictly met experimentally if the experiments were performed with red blood cell ghosts. The parameters used for the computation of the curves are listed in Table 1. The unidirectional anion fluxes were measured at Donnan equilibrium by means of radioactive isotopes, i.e., under conditions where no anion net flux takes place (*cf. Materials and Methods*).

Table 1. Parameters used for the computer simulation of the flux curves shown in Figs. 6–9

	σ_{max} amp · sec · cm^{-2}	K M	$K_{s(SO_4)}$ M	$K_{s(Cl)}$ M
Side′	1.6×10^{-4}	1×10^{-7}	1×10^{2}	1×10^{-1}
Side″	1.6×10^{-6}	1×10^{-7}	1×10^{-1}	1×10^{-1}

Fig. 6 exhibits a comparison between computer simulated and experimentally determined sulfate flux curves. The concentration-dependence of the experimentally determined unidirectional sulfate flux (Fig. 6*b*) displays a concentration maximum shifting from about 150 mM at pH 6.3 (25 °C) to about 300 mM at pH 8.5 (25 °C). The apparent half-saturation constants were found to increase from 30 mM (pH 6.3) to approximately 120 mM (pH 8.5). The pH-maximum of the unidirectional sulfate flux (Fig. 6*d*) is located between pH 6.2–6.4 (25 °C) and is little affected by changes of the sulfate concentrations. The sulfate flux experiments were performed in the presence of amphotericin B. At low concentrations (5 μg/ml) amphotericin B has no effect on the sulfate flux [57]. It is evident from Fig. 6 that the computer simulated flux curves are qualitatively in accordance with the experimental results.

A comparison between the theoretical and the experimental flux/concentration and flux/pH curves for the unidirectional chloride flux is shown in Fig. 7. According to the studies of Dalmark [9], the concentration maximum of the unidirectional chloride flux measured at 0 °C shifts from about 100 mM at pH 6.2 to about 300 mM at pH 9.2 (Fig. 7*b*). Concomitantly, the apparent half-saturation constant increases from 10 mM (pH 6.2) to 70 mM (pH 9.2). The concentration-dependence of the computer simulated flux is shown in Fig. 7*a*. In contrast to the pH-dependence of the unidirectional sulfate flux, the pH-dependence of the unidirectional chloride flux is strongly influenced by the chloride concentration. The pH-maximum of the flux curves is most pronounced at low chloride concentrations and gradually disappears as the chloride concentration is raised (Fig. 7*d*). The computer simulated pH-dependence of the flux curves (Fig. 7*c*) and the experimentally observed pH-dependence (Fig. 7*d*) display the same type of behavior.

Fig. 8 shows the effect of increasing chloride concentrations upon the concentration response of the unidirectional sulfate flux. The apparent

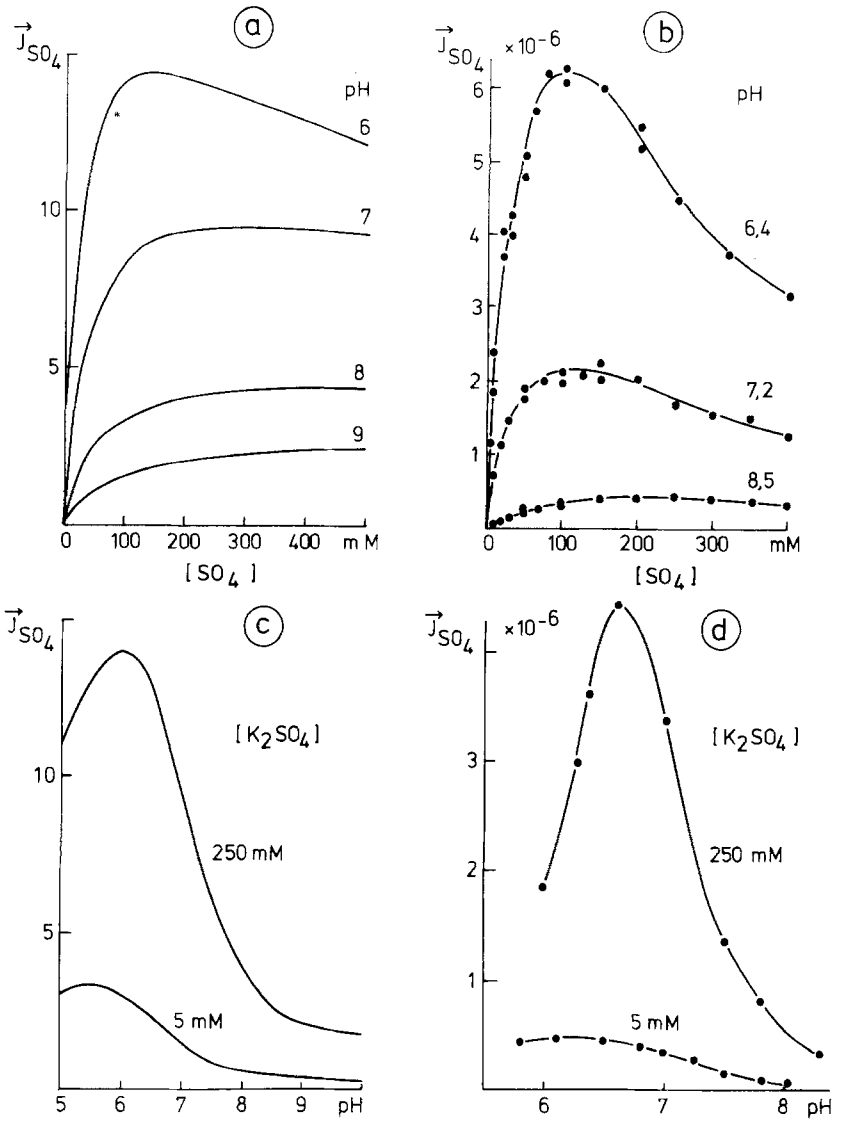

Fig. 6. Comparison between computer simulated and the experimentally observed concentration-dependence and pH-dependence of the unidirectional sulfate flux. (*a*): Computer simulated concentration-dependence. The unidirectional sulfate flux $\vec{J}_{SO_4}$ (arbitrary units) is plotted *vs.* the sulfate concentration $[SO_4]$ (mM). (*b*): Experimentally observed concentration-dependence of the unidirectional sulfate flux (amphotericin B-treated red blood cells, 25 °C). The unidirectional flux $\vec{J}_{SO_4}$ (moles · min^{-1} · g cells dry wt^{-1}) is plotted *vs.* the extracellular sulfate concentration $[SO_4]$ (mM). pH is indicated at the respective curves. (*c*): Computer simulated pH-dependence of the unidirectional sulfate flux. The flux $\vec{J}_{SO_4}$ (arbitrary units) is plotted *vs.* pH. (*d*): Experimentally observed pH-dependence of the unidirectional sulfate flux. The flux $\vec{J}_{SO_4}$ (moles · min^{-1} · g cells dry wt^{-1}) is plotted *vs.* pH. The sulfate concentration is indicated in the figures. Composition of the incubation solution: 5 µg/ml amphotericin B, 60 mM sucrose, 25 mM K-phosphate buffer plus *x* mM K_2SO_4 as indicated in the figures. Cell concentration: 10% (w/v). The computer simulated flux curves were calculated by means of Eqs. (5), (6), (7) and (19). The parameters used for the computation are listed in Table 1

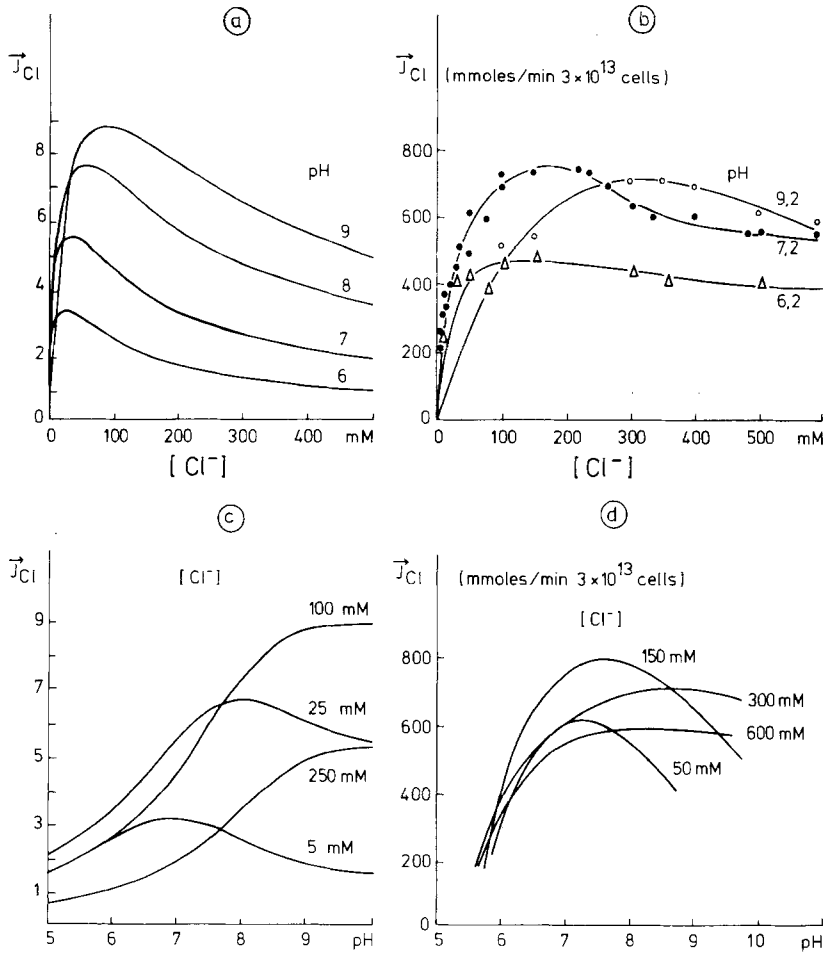

Fig. 7. Comparison between the computer simulated and the experimentally determined unidirectional fluxes of chloride. The experimental data were taken from Dalmark [9]. (*a*): Computer simulated concentration-dependence of the unidirectional cloride flux. The flux $\vec{J}_{Cl}$ (arbitrary units) is plotted *vs.* the chloride concentration $[Cl^-]$ (mM). (*b*): Experimentally observed concentration-dependence of the unidirectional chloride flux. The flux $\vec{J}_{Cl}$ (mmoles/min $\cdot 3 \times 10^{13}$ cells) is plotted as a function of the extracellular chloride concentration $[Cl^-]$ (mM). pH is indicated at the respective curves. Composition of the incubation solution: 5–600 mM KCl, 1 mM NaCl, 25 mM sucrose. (*c*): Computer simulated pH-dependence of the unidirectional chloride flux. The flux $\vec{J}_{Cl}$ (arbitrary units) is plotted *vs.* pH. (*d*): Experimentally determined pH-dependence of the unidirectional chloride flux. The flux $\vec{J}_{Cl}$ (mmoles/min $\cdot 3 \times 10^{13}$ cells) is plotted *vs.* pH. The chloride concentration $[Cl^-]$ is indicated at the respective curves. Composition of the incubation solution: 5–600 mM KCl, 1 mM NaCl, 25 mM sucrose. The experiments were conducted with nystatin treated red blood cells at 0 °C. The cell concentration was 1 % (w/v). For the computation of the theoretical curves, Eqs. (5), (6), (7) and (19) were used. The parameters are listed in Table 1

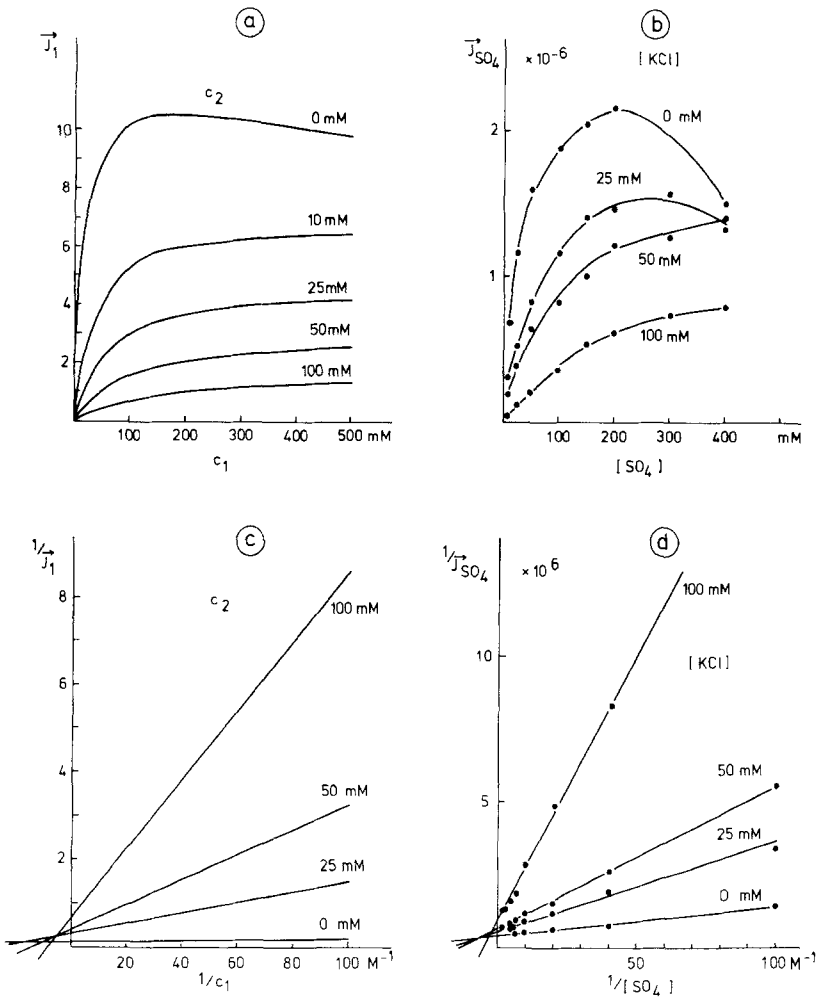

Fig. 8. The effect of chloride on the concentration-dependence of the unidirectional sulfate flux. (*a*): Computer simulated curves. The unidirectional flux $\vec{J}_1$ (arbitrary units) is plotted *vs.* the concentration c_1 (mM) of the anion species 1. pH 7.0. Concentrations of the 2nd anion species c_2 (mM) as indicated in the figure. (*b*): Experimentally determined flux/concentration curves. The unidirectional sulfate flux $\vec{J}_{SO_4}$ (moles · min^{-1} · g cells dry wt^{-1}) is plotted as a function of the extracellular sulfate concentration [SO_4] (mM); pH 7.2, 25 °C. The KCl concentration is noted at the respective curves. (*c*): Computer simulated Lineweaver-Burk plot. The concentration range from 10–200 mM (Fig. 8*a*) was used. (*d*): Lineweaver-Burk plot made from the data shown in *b*. The ascending branches of the flux/concentration curves were used. The experiments were conducted with a 10% cell suspension at 25 °C. The red cells were treated with amphotericin B. Composition of the incubation solution: 5 µg/ml amphotericin B, 25 mM K-phosphate buffer, 60 mM sucrose, K_2SO_4 concentration and KCl concentration as indicated in the figure. The computations were made by using Eqs. (5), (6), (7) and (19). The parameters used for the computation are listed in Table 1

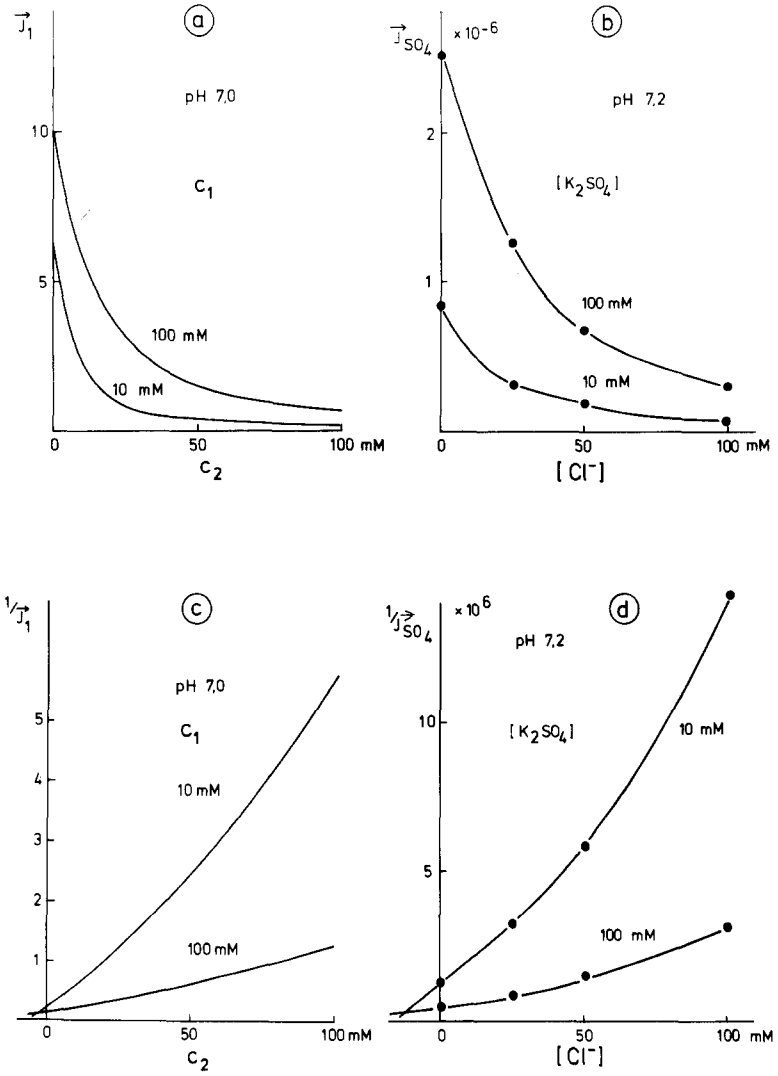

Fig. 9. The inhibition of the unidirectional sulfate flux by chloride. (*a*): Computer simulated dose-response curves. The unidirectional flux $\vec{J}_1$ (arbitrary units) of the 1st anion species is plotted as a function of the concentration c_2 (mM) of the 2nd anion species. Concentrations c_1 of the 1st anion species as indicated in the figure. (*b*): Experimentally determined dose-response curves. The unidirectional sulfate flux $\vec{J}_{SO_4}$ (moles · min^{-1} · g cells dry wt^{-1}) is plotted *vs.* the extracellular chloride concentration [Cl^-] (mM). pH and sulfate concentrations [K_2SO_4] (mM) as indicated in the figure. (*c*): Computer simulated Dixon plot. (*d*): Dixon plot made from the experiments shown in *b*. The sulfate measurements were performed with amphotericin B-treated red blood cells at 25 °C, 10% (w/v) cell suspension. Composition of the incubation solutions: 5 μg/ml amphotericin B, 25 mM K-phosphate buffer, 60 mM sucrose, K_2SO_4 concentrations and KCl concentrations as denoted in the figure. Eqs. (5), (6), (7) and (19) were used for the computation of the flux curves. $z_1 = -2$; $z_2 = -1$; other parameters as in Table 1

half-saturation constant of the unidirectional sulfate flux (25 °C) increases from 25 to 285 mM as the chloride concentration is raised from 0 to 100 mM. The position of the concentration maximum of the unidirectional sulfate flux shifts toward higher sulfate concentrations and finally the concentration maximum disappears (Fig. 8*a* and 8*b*). It should be mentioned in this context that corresponding results were obtained by Dalmark [10] who studied the action of bicarbonate and halide anions on the concentration-dependence of the chloride flux. The Lineweaver-Burk plots made from the ascending branches of the flux/concentration curves (Fig. 8*c* and *d*) show a linear relation between the reciprocal sulfate flux and the reciprocal sulfate concentration. The straight lines do not intersect at one point.

In Fig. 9 the inhibition of the unidirectional sulfate flux by chloride is shown. Fig. 9*a* and *b* exhibit the computed and the experimentally determined dose-response curves, Fig. 9*c* and *d* show the corresponding Dixon plots. As already mentioned, the relation between the reciprocal of the sulfate flux and the chloride concentration is not linear as should be expected for pure competition. The elongation of the curves intersect distinctly above the abscissa.

Figs. 6–9 demonstrate that the proposed model is capable of describing the basic features of the sulfate and the chloride transport at Donnan equilibrium. Although no attempts were made to fit the experimental data to the above model, there are two interesting results that should be mentioned. Firstly, it was only possible to simulate the experimentally observed features of the unidirectional sulfate flux and the unidirectional chloride flux by making the membrane asymmetric ($\sigma'_{max} \neq \sigma''_{max}$). Secondly, it was sufficient to change one single dissociation constant K_{si} in order to convert the system from a "sulfate transport system" into a "chloride transport system".

Discussion

Membrane Structure

The present paper is concerned with the mechanism of the anion transport across the red blood cell membrane. During recent years, the kinetics of the anion transport across the red cell membrane has been extensively studied in several laboratories. Despite considerable progress in the biochemical field of membrane research, the mechanism of the

anion transport is not yet understood. This is partially due to a lack of detailed information on the membrane structure and partially due to a lack of new theoretical concepts which could be subjected to a rigorous experimental test. Therefore, in this paper attempts were made to develop an anion transport model taking into account our present knowledge of the membrane ultrastructure.

The erythrocyte membrane is visualized as a mosaic membrane consisting of a lipid bilayer which is interrupted by the insertion of large protein molecules [58]. These protein molecules are supposed to penetrate the cellular membrane and to be in contact with the outer and the inner membrane surfaces. According to a suggestion by Parsegian [44], the proteins spanning the cell membrane may serve as dielectric pores responsible for the ion transport across the cell membrane.

The concept of dielectric pores appears to be consistent with modern concepts of the membrane ultrastructure emerging from freeze-etching studies of the red cell membrane. The cleavage of the erythrocyte membrane along its inner hydrophobic junction reveals a smooth lipid matrix interrupted by a large number of inclusions. These inclusions have a diameter of 80 to 200 Å and correspond to proteins which span the cell membrane [40, 58, 68]. The hypothesis of dielectric pores is further supported by recent biochemical studies indicating that a membrane protein with a molecular weight of 95,000 daltons (95 K) plays a crucial role in anion transport across the erythrocyte membrane. However, the precise function of the 95K membrane protein is still uncertain [5–7, 39, 46, 50, 51, 74].

In the present paper, the concept of dielectric pores was adopted for the description of the anion transport across the red blood cell membrane. The transport of anions across the membrane is assumed to take place by a diffusion process which is regulated by superficial anion adsorption sites. For the description of the diffusion process, the formalism of the transition state theory was employed. The description of the anion transport model is based upon a number of assumptions which are delineated in the results section. In the subsequent sections, the experimental basis of the assumptions underlying the present transport model will be discussed in detail.

Adsorption of Anions to the Membrane Surfaces

The first step of the anion transport across the red blood cell membrane is the adsorption of the anion to one of the membrane

surfaces. It appears from a number of experimental results that both chemical adsorption forces (short range forces) and electrostatic adsorption forces (long range forces) are involved in the binding of anions to the membrane surfaces. In this paper, the membrane surfaces were treated as electrically charged surfaces which bear a limited number of anion adsorption sites. Furthermore, it was assumed that small inorganic anions interact with the same anion binding sites and are transported by the same transport system.

The saturation of the chloride [8, 9, 28, 71] and of the sulfate [29, 55, 57] flux indicates that both anion species interact with a limited number of membrane sites. However it remains unclear from these experiments whether the anion binding sites are located on the outer membrane surface, on the inner membrane surface or whether they are positioned in the interior of the red blood cell membrane. Interesting information concerning the location of the anion adsorption sites is obtained from studies with nonpenetrating inhibitors. In order to cause an inhibition, the inhibitor molecule has to be bound either directly to the anion adsorption site or to its immediate vicinity. Nonpenetrating inhibitors such as phlorizin and DAS (4,4′-Diacetamido-stilbene-2,2′-disulfonic acid) cause a strong inhibition of the sulfate and of the chloride exchange if acting on the outer membrane surface, but they were found to be completely ineffective if applied to the inner membrane surface [34, 39, 46, 56, 74]. Contrastingly, APMB (2-(4′-aminophenyl)-6-methylbenzenethiazol-3′,7-disulfonic acid) was found to produce an inhibition of the anion transport at either membrane surfaces [39, 74]. From these results the following conclusions can be drawn: (i) There are anion binding sites at the outer *and* at the inner membrane surfaces. (ii) The anion binding sites at the inner and at the outer membrane surfaces seem to be different. (iii) The anion binding sites have to be positioned on the membrane surfaces, where they are accessible to the inhibitor molecules.

According to our experiments [57] and to the experiments of Dalmark [10], the sulfate flux and the chloride flux are competitively inhibited by small inorganic anions. In contrast amphiphilic inhibitors such as phlorizin display a noncompetitive type of inhibition [20, 54]. The mutual competition between sulfate and chloride suggests that both anion species become adsorbed to the same membrane sites. Anions which carry the same electrical charge differ considerably with respect to their inhibitory action on the sulfate and the chloride transports [12, 57, 69]. These differences have to be attributed to individual properties of

the respective anion species, suggesting that short range forces participate in the binding of anions to the membrane surfaces. No correlation between the penetration rate of the inhibiting anion and its inhibitory action on the chloride transport was observed [10, 12, 57, 69]. This observation rules out the possibility that two anions compete for a common binding site within a narrow pore and supplies further evidence to the above conclusions that the anion adsorption sites are located on the membrane surfaces.

The adsorption of anions to the membrane surfaces seems to be supported by electrostatic forces. It was assumed that ammonium groups at the membrane surfaces set up an electrical potential which contributes to the adsorption of anions to the anion adsorption sites. This inference is mainly based upon inhibitor studies with amino group reagents which are powerful inhibitors of the anion permeability [5–7, 35, 45–50, 52]. Most of the amino groups taking part in the regulation of the anion permeability seem to be located on the 95 K protein at the outer membrane surface and can be labelled by nonpenetrating amino group reagents such as SITS (4-acetamido-4′-isothiocyanostilbene-2,2′-disulfonic acid) [5–7, 35, 37, 50, 52, 74]. There is some evidence, that amino groups are also present at the inner membrane surface, although their significance for the anion transport is not yet clear. Pretreatment of red blood cells with SITS considerably reduces the binding of the amino group reagent DNFB (1-fluoro-2,4-dinitrophenol) to the 95 K protein, but does not completely prevent this binding [46, 74]. In contrast to SITS, DNFB can penetrate the erythrocyte membrane. One might speculate that the amino groups which are not protected against DNFB labelling by SITS are positioned on the inner membrane surface.

For the computation of the surface potential, the Gouy-Chapman theory of the electrical double layer was employed (*cf. Results*, Eqs. (3)–(5). The Gouy-Chapman theory is well known and need not be discussed except for noting some deficiencies inherent in the theory: (i) The Gouy-Chapman theory treats the membrane surfaces as planar and perfectly impermeable surfaces with a surface charge which is uniformly distributed over the membrane surface. It neglects consequences of discreetness and molecularity of the solutions and of the membrane surfaces and ignores to a certain extent, the structural heterogeneity of the membrane surfaces. These refinements however, can only be taken into consideration if the ultrastructure of the membrane surfaces is known. (ii) Furthermore, the Gouy-Chapmyn theory disregards the contribution of the electrical charge of contact-adsorbed anions to the total surface charge.

This can only be done if the number of contact-adsorbed anions at the membrane surface is much smaller than the number of fixed charges (positive + negative fixed charges) within this particular membrane area. Otherwise the Stern theory of the electrical double layer should be used, which gives essentially similar results, but introduces additional mathematical difficulties [54].

Transport of Anions across the Membrane

Recent biochemical studies have shown that the 95 K membrane protein plays a decisive role in anion transport across the red blood cell membrane. The 95 K protein can be extracted from the erythrocyte membrane and was found to enhance the sulfate permeability of lecithin vesicles [51]. According to the investigations of Steck [60, 61] and Müller and Morrison [43], the 95 K protein spans the red cell membrane and seems to be in contact with the outer and with the inner membrane surface. The true function of the 95 K protein is not yet understood, but it could easily form a dielectric pore which facilitates the anion transport across the red blood cell membrane.

The transport of anions across the erythrocyte membrane is supposed to occur by ionic diffusion through dielectric pores. The fundamental process in diffusion is the jumping of an ion across an energy barrier. The frequency at which this occurs is determined by the free energy of activation ΔF_i, which is the change in energy necessary for the ith ion to pass from its current equilibrium position in front of the barrier to the top of the energy barrier. The rate constant $\vec{k}_{i0}$ for a diffusive jump can therefore be written as [16, 22, 27]:

$$\vec{k}_{i0} = \kappa(kT/h) \cdot \exp(-\Delta F_i/kT). \tag{26}$$

$\vec{k}_{i0}$ is the basic rate constant if the electrical potential across the respective barrier is zero, k is the Boltzman constant, h the Planck's constant, T the absolute temperature, and κ is the transmission coefficient which is usually equal to unity. If the dielectric pore is sufficiently wide, image forces, arising from the walls of the pore can be neglected [67] and the energy profile of the pore can be expressed as shown in Fig. 2.

At a first approximation, the free energy of activation for the transport of an anion across a dielectric pore is determined by the self-energy of the anion within the pore. According to the Born equation [3],

the self-energy of the anion within the pore is determined by the dielectric constant of the pore region:

$$\Delta F_i = \frac{(z_i q)^2}{2 r_i} (1/\varepsilon_m - 1/\varepsilon_s). \tag{27}$$

ε_m and ε_s are the dielectric constants of the pore and of the aqueous solution, respectively, and r_i is the radius of the ith ion. The other symbols have their usual meanings. Inserting the cristallic radii for sulfate (2.5 Å) and for chloride (1.81 Å), the free energy of activation is obtained as a function of the dielectric constant ε_m of the pore region (Table 2).

A crude estimate of the free energies of activation can be made from the flux measurements. The unidirectional flux $\vec{J}_i$ of the ith anion is given by Eq. (18). For a symmetric membrane and a single electrolyte, Eq. (18) can be rewritten as:

$$\vec{J}_i = \vec{k}_{i0} N_s (N_i/N_s)(1 - N_i/N_s). \tag{28}$$

$\vec{k}_{i0}$ ($\sec^{-1}$) is the translocation rate as defined by Eq. (26), N_s (cm^{-2}) is the maximal concentration of contact-adsorbed anions at the membrane surfaces, and N_i/N_s is the fraction of occupied sites. As shown in the results section, a maximal flux is reached at a half-saturation of the membrane surfaces. At half-saturation $N_i/N_s = 0.5$ and the term $(N_i/N_s)(1 - N_i/N_s)$ in Eq. (28) is equal to 0.25. Thus, if the maximal flux of an anion species can be experimentally determined and if N_s is known, Eq. (28) can be used for a computation of the translocation rate $\vec{k}_{i0}$.

Table 2. Free energies of activation obtained from the Born equation (Eq. (27))[a]

ε_m	ΔF_{SO_4} kcal/moles	ΔF_{Cl} kcal/moles
2	129.8	44.8
5	49.9	17.2
10	23.3	8.0
15	14.4	4.9
20	9.9	3.4
25	7.2	2.5

[a] The following parameters were used: $r_{SO_4} = 2.5$ Å, $r_{Cl} = 1.81$ Å, $\varepsilon_s = 78$.

The maximal concentration of contact-adsorbed anions N_s is determined by the number of anion adsorption sites on the membrane surfaces. Rothstein and Cabantchik [50] studied the relation between the inhibition of the sulfate exchange and the binding of ^{3}H-labelled DIDS to the erythrocyte membrane. They found that 2.5×10^5 molecules of DIDS per cell were bound to the 95 K protein. From their results they concluded that the number of DIDS binding sites per cell is equal to the number of anion adsorption sites. Passow, Fasold, Zaki, Schuhmann and Lepke have observed a much higher number of DIDS binding sites per cell. According to their results, the number of DIDS binding sites amount to 1.3×10^6 per cell [37, 46, 74]. Thus, a number of 1.3×10^6 sites/cell has to be considered as an upper limit for the number of anion adsorption sites on the membrane surface.

According to our results [61], the maximal experimentally observed sulfate flux is 1.3×10^{-17} moles $\times$ sec$^{-1} \times$ cell^{-1} at 37 °C (pH 6.2) and 3.4×10^{-18} moles $\times$ sec$^{-1} \times$ cell^{-1} at 25 °C (pH 6.2), respectively. Using Eq. (27) for the estimation of k_{i0} and assuming a number of 1×10^6 anion adsorption sites per cell, we end up with a translocation rate of 31 sec^{-1} at 37 °C and of 8 sec^{-1} at 25 °C for sulfate. Brahm [4] reported a maximal unidirectional chloride flux of 8×10^{-14} moles $\times$ sec$^{-1} \times$ cell^{-1} (38 °C; pH 7.4), which according to the above assumptions yields a translocation rate for chloride of 1.9×10^5 sec^{-1}. According to Eq. (26), a free energy of activation of 16.2 kcal/mole for the sulfate transport and of 10.8 kcal/mole for the chloride transport is obtained. (The frequency factor kT/h (Eq. (26)) is 6.5×10^{12} sec^{-1} at 37 °C and 6.2×10^{12} sec^{-1} at 25 °C.)

A comparison of the free activation energies as calculated from the flux measurements and of the free activation energies as computed by means of the Born equation (Table 2) reveals that the dielectric constant of the pores should be between 10 and 15. This value is considerably higher than the dielectric constant of black lipid membranes ($\varepsilon_m = 2$; [31, 32, 63]) and appreciably lower than the dielectric constant of water ($\varepsilon \cong 80$). The dielectric constant of the pore region is slightly higher than the dielectric constant of the entire red blood cell membrane which, according to the capacitance measurements of Fricke [17–19], amounts to about 10. A dielectric constant between 10 and 15 is also consistent with the measurements of Takashima and Schwann [64] who found dielectric constants for proteins ranging from very low values for the dry crystal up to values comparable to the dielectric constant of water if the water content of the protein is only increased up to 5%.

Table 3. Free energies of activation ΔF_i, free enthalpies of activation ΔH_i and free entropies of activation ΔS_i. The free energies of activation for sulfate and for chloride were computed by means of Eqs. (26) and (28) from the data of Schnell, Gerhardt and Schöppe-Fredenburg [57] and the data of Brahm [4]. The free enthalpies of activation were taken from Lepke and Passow [37] and from Brahm [4]

Anion	ΔF_i kcal/moles	ΔH_i kcal/moles	ΔS_i kcal · moles^{-1} · deg^{-1}
$SO_4^=$	16.2	33	$5.4 \cdot 10^{-2}$
Cl^-	10.8	22	$3.6 \cdot 10^{-2}$

The relation between the free energy of activation ΔF_i, the free enthalpy of activation ΔH_i and the free entropy of activation ΔS_i is given by the Gibbs equation:

$$\Delta F_i = \Delta H_i - T\Delta S_i \tag{30}$$

with T being the absolute temperature. ΔH_i can be determined from the temperature dependence of the unidirectional fluxes by means of the Arrhenius procedure. Within a temperature range of 20–38 °C, the free enthalpy of activation for the chloride transport is 22 kcal/mole [4]. The free activation enthalpy for the sulfate transfer at the same temperature is about 33 kcal/mole [38, 53, 69]. Using ΔF_i as determined by means of the flux measurements and ΔH_i as obtained by the Arrhenius procedure, the free entropy of activation ΔS_i can be computed by making use of the Gibbs equation. The results are listed in Table 3.

Computer Simulation of the Flux Curves

As shown in this paper, it is possible to simulate the experimentally observed concentration-response and pH-response of the unidirectional fluxes of sulfate and of chloride (Figs. 6 and 7) by using the same membrane parameters (σ_{max} and K) for both anion species and only changing those parameters (K_{si}) which depend upon the chemical properties of the transported anion species.

For the computer simulation of the flux curves, a fixed charge density σ_{max} between 1.6×10^{-6} and 1.6×10^{-4} amp · sec · cm^{-2} was used, corresponding to a charge density of 1 elementary charge/1,000 Å^2 and 1 elementary charge/10 Å^2. These values are in accordance with the values reported in the literature. Lakshminarayanaiah and Murayama [36]

have reported surface charge densities for nerve and muscle membranes ranging from 1 elementary charge/2,000 Å^2 up to 1 elementary charge/40 Å^2. A charge density of 1 elementary charge/10 Å^2 certainly has to be considered as an upper limit. In previous studies on the sulfate [20, 38, 45] and on the phosphate transport [14] across the erythrocyte membrane, a fixed charge density of approximately 3 moles/liter was employed in order to fit the experimental data. Assuming a thickness of the membrane water interface of about 10 Å, a fixed charge density of 3 moles/liter would correspond to a surface charge density of 1 elementary charge/55 Å^2. It might be more realistic to assume that a mixed population of positive and negative charges exists on the membrane surfaces. If necessary, extensions of the model in this direction can be easily made, but they considerably increase the mathematical difficulties for the calculations of the surface potentials.

For the calculation of the surface potentials, ionization constants of 1×10^{-7} moles/liter were inserted. A pK of 7 is justified if α-amino groups, histidino or guanido groups are responsible for the surface potential in this particular membrane area. This assumption is compatible with the results obtained with group specific reagents, suggesting that dissociable cationic groups, presumably amino groups, are directly involved in the regulation of the anion permeability. In the other hand, it should be mentioned that the apparent pK's as obtained from the flux/pH curves are difficult to interpret since they might reflect the behavior of a mixed population of cationic and anionic groups.

The site-anion dissociation constants K_{si} used for the simulation of the flux curves range from 0.1 moles/liter to 100 moles/liter. A value of 100 moles/liter appears to be extremely high. However, K_{si} is determined by the chemical adsorption forces which for small inorganic anions may, in fact, be extremely low. A surface potential of 100 mV would reduce these values by a factor of 600 for divalent and by a factor of approximately 25 for monovalent anions. Thus, the apparent half-saturation constants would be of an order of magnitude which is experimentally observed.

No attempts were made to fit the experimental data to the model. Therefore, the parameters used for the computation of the curves must not be overinterpreted. In order to fit the experimental data in the presence of a single anion species, seven independent parameters are required, and if a second anion species is present, two additional parameters are necessary. A proper fit of the experimental data therefore seems to be only reasonable if the order of magnitude of some of the parameters involved can be determined by independent methods.

There are two results which are of great theoretical importance. As pointed out before, the energy profile of the penetration route does not only determine the absolute flux rates, but, in addition, it determines the magnitude of the site-anion dissociation constant K_{si}. As shown in Fig. 4, K_{si} profoundly affects the concentration-response and the pH-response of the unidirectional fluxes. In general, the energy profiles for different anion species differ conspiciously. Thus, we have to expect differences in the concentration-dependence and the pH-dependence for the unidirectional fluxes of different anion species, even if the anions are transported by the same anion transport system. Furthermore, we could only simulate the experimental concentration-responses and pH-responses of unidirectional fluxes of sulfate and chloride by making the membrane asymmetric. The latter assumption is consistent with the general opinions concerning the membrane ultrastructure.

Comparison between Carrier and Pore Transport Mechanism

In this paper the anion transport across the red blood cell membrane was considered to occur by ionic diffusion through dielectric pores which traverse the erythrocyte membrane. As an alternative approach, the anion transport across the erythrocyte membrane can be visualized to be mediated by a mobile carrier [8, 9, 25, 26, 28, 70]. Although it is theoretically possible to distinguish between a carrier and a pore transport mechanism [41, 42], at the moment we have no experimental results which would permit an unequivocal discrimination between both transport mechanisms. It seems that most of the experimental results can be matched by both transport concepts if suitable extensions are made.

Studies with artificial lipid bilayers have shown that pores in general, have much higher turn-over numbers than carriers. Stark and Läuger [59] and Bamberg and Läuger [1] studied the action of the antibiotics valinomycin and gramicidin A on the conductivity of black lipid membranes. From their data the turn-over numbers can be computed. For gramicidin A, which forms pores, turn-over numbers of approximately 1×10^7 sec^{-1} were obtained, whereas for valinomycin, which acts as a carrier, turn-over numbers of about 1×10^4 sec^{-1} at 20 °C were found. Brahm [4] has reported a turn-over rate of 2×10^5 sec^{-1} for the chloride exchange flux at 38 °C and pH 7.4. Since the Arrhenius activation energy for the chloride transport is approximately 22 kcal $\times$ mole$^{-1} \times$ deg^{-1}, this would correspond to a turn-over number of 2×10^4 sec^{-1} at 20 °C which still seems to be consistent with the turn-over numbers for a carrier transport system.

On the one hand, it seems difficult to find a membrane constituent that could act as a mobile carrier. Usually the effective membrane thickness is supposed to be approximately 50 Å. If the 95-K protein would act as a carrier, the molecule would have to undergo conformational changes which would result in a displacement of the anion binding group(s) over a distance of about 50 Å. Conformational changes resulting in a displacement of these binding groups over such a distance are unlikely to occur under physiological conditions, yet they cannot be excluded with certainty.

Toyoshima and Thompson [65, 66] have reported an electrically silent chloride transport in lipid bilayers made of phosphatidylcholine. They concluded that the chloride transport is associated with a "flip-flop" of phosphatidylcholine which presumably acts as a chloride carrier. Since Gruber and Deuticke [24] and Wieth *et al.* [72] have observed a correlation between the anion permeability and the phosphatidylcholine content of red blood cells of different mammalian species, one might speculate that not the membrane proteins but the membrane lipids are responsible for the anion transport across the erythrocyte membrane. However, the chloride exchange permeability of the lipid bilayer amounts to approximately 6.8×10^{-8} cm · sec^{-1} (20 °C). It is about 4–5 orders of magnitude smaller than the chloride permeability of human red cells [9] under comparable conditions. Therefore, it appears unlikely that this transport mechanism is responsible for the transport of anions in red blood cells.

In spite of our present incapacity to distinguish between a carrier and a pore transport mechanism, there are basic differences between both transport mechanisms. The carrier hypothesis assumes the anion transport to be associated with the movement of a membrane constituent which forms an electrically neutral complex with the transported anion. The pore concept, on the other hand, assumes that only the transported anion is moving, whereas the membrane structures are fixed in their positions. The asymmetric inhibition of the anion transport caused by the inhibitors phlorizin, DAS and APMB [34, 39, 46, 56, 74] suggests that the anion binding sites at the inner and outer membrane surfaces are different. These findings can be explained easily on the basis of a pore transport mechanism, however, they do not provide conclusive evidence against a carrier transport mechanism. These results would probably also be consistent with a highly asymmetric carrier system.

This work was supported by the Deutsche Forschungsgemeinschaft. The skilful technical assistance of Mrs. E. Besl and A. Manz is gratefully acknowledged. I wish to

thank Prof. C. Albers and Prof. K.D. Heckmann for their support of my work. In particular, I am indebted to R. von der Mosel for helpful comments during the preparation of the manuscript.

References

1. Bamberg, E., Läuger, P. 1973. Channel formation kinetics of gramicidin A in lipid bilayer membranes. *J. Membrane Biol.* **11**:177
2. Beneš, I., Kolinská, J., Kotyk, A. 1972. Effect of phloretin on monosaccharide transport in erythrocyte ghosts. *J. Membrane Biol.* **8**:303
3. Born, M. 1920. Volumen und Hydrationswärme von Ionen. *Z. Physik* **1**:45
4. Brahm, J. 1975. Chloride permeability in human red cells at 0–38 °C. Vth International Biophysics Congress Copenhagen (Abstr.) p. 319
5. Cabantchik, Z.I., Rothstein, A. 1972. The nature of the membrane sites controlling anion permeability of human red blood cells as determined by studies with disulfonic stilbene derivatives. *J. Membrane Biol.* **10**:311
6. Cabantchik, Z.I., Rothstein, A. 1974*a*. Membrane proteins related to anion permeability of human red blood cells. I. Localization of disulfonic stilbene binding sites in proteins involved in permeation. *J. Membrane Biol.* **15**:207
7. Cabantchik, Z.I., Rothstein, A. 1974*b*. Membrane proteins related to anion permeability of human red blood cells. II. Effects of proteolytic enzymes on disulfonic stilbene sites of surface proteins. *J. Membrane Biol.* **15**:227
8. Cass, A., Dalmark, M. 1973. Equilibrium dialysis of ions in nystatin-treated red cells. *Nature New Biol.* **244(132)**:47
9. Dalmark, M. 1975. Chloride transport in human red cells. *J. Physiol. (London)* **250**:39
10. Dalmark, M. 1976. Effects of halides and bicarbonate on chloride transport in human red blood cells. *J. Gen. Physiol.* **67**:223
11. Deuticke, B. 1967. Über die Kinetik der Phosphat-Permeation in den Menschenerythrozyten bei Variation von extracellulärer Phosphat-Konzentration, Anionen-Milieu und Zellvolumen. *Pfluegers Arch.* **296**:21
12. Deuticke, B. 1970. Anion permeability of the red blood cells. *Naturwissenschaften* **57**:172
13. Deuticke, B. 1972. Passive anion transfer across the red cell membrane and its alteration by amphiphilic compounds. *In:* Biomembranes, Vol. 3, Passive Permeability of Cell Membranes. F. Kreuzer and J.F.G. Slegers, editors. p. 381. Plenum Press, New York-London
14. Deuticke, B., Dierkesmann, R., Bach, D. 1968. Neuere Studien zur Anionen-Permeabilität menschlicher Erythrozyten. *In:* Metabolism and membrane permeability of erythrocytes and thrombocytes. E. Deutsch, E. Gerlach, and K. Moser, editors. p. 430. Thieme-Verlag, Stuttgart
15. Deuticke, B., Gerlach, E. 1967. Beeinflussung von Form und Phosphat-Permeabilität menschlicher Erythrozyten durch hämolysive Benzol-Derivate und pharmakologisch aktive Substanzen. *Klin. Wochenschr.* **224**:977
16. Frenkel, J.I. 1946. Kinetic Theory of Liquids. Oxford University Press, London-New York
17. Fricke, H. 1925. The electrical capacity of suspensions with special reference to blood. *J. Gen. Physiol.* **9**:137
18. Fricke, H. 1933. The electrical impedance of suspensions of biological cells. *Cold Spring Harbor Symp. Quant. Biol.* **1**:117
19. Fricke, H., Curtis, H.J. 1935. The electrical impedance of hemolysed suspensions of mammalian erythrocytes. *J. Gen. Physiol.* **18**:821

20. Gerhardt, S., Schöppe-Fredenburg, A., Schnell, K.F. 1973. Inhibition of the sulfate transfer in human erythrocytes. *In:* Erythrocytes, Thrombocytes, Leukocytes. E. Gerlach, K. Moser, E. Deutsch and W. Wilmans, editors. p. 87. Thieme-Verlag Stuttgart
21. Gerlach, E., Deuticke, B., Duhm, J. 1964. Phosphatpermeabilität und Phosphatstoffwechsel menschlicher Erythrozyten und Möglichkeiten ihrer experimentellen Beeinflussung. *Pfluegers Arch.* **280**:243
22. Glastone, S., Laidler, K.J., Eyring, H. 1941. The Theory of Rate Processes. McGraw-Hill, New York
23. Graham, D.C. 1947. The electrical double layer and the theory of electrocapillarity. *Chem. Rev.* **41**:441
24. Gruber, W., Deuticke, B. 1973. Comparative aspects of phosphate transfer across mammalian erythrocyte membranes. *J. Membrane Biol.* **13**:19
25. Gunn, R.B. 1972. A titrable carrier model for both mono- and divalent anion transport in human red cells. *In:* Oxygen Affinity of Hemoglobin and Red Cell Acid Base Status. M. Rørth and P. Astrup, editors. p. 823. Munsgaard, Copenhagen
26. Gunn, R.B. 1973. A titrable carrier for monovalent and divalent inorganic anions in red blood cells. *In:* Erythrocytes, Thrombocytes, Leukocytes. E. Gerlach, K. Moser, E. Deutsch and W. Wilmans, editors. p. 77. Thieme-Verlag, Stuttgart
27. Gunn, R.B., Cooper, J.A., Jr. 1975. Effect of local anesthetics on chloride transport in erythrocytes. *J. Membrane Biol.* **25**:311
28. Gunn, R.B., Dalmark, M., Tosteson, D.C., Wieth, J.O. 1973. Characteristics of chloride transport in human red blood cells. *J. Gen. Physiol.* **61**:185
29. Gunn, R.B., Hartly, O.N., Horton, J.M. 1974. Sulfate transport in human red blood cells: Concentration dependence of the sulfate flux. *Fed. Proc.* **33**:2086 *(Abstr.)*
30. Gunn, R.B., Tosteson, D.C. 1971. The effect of 2,4,6-trinitro-m-cresol on cation and anion transport in sheep red blood cells. *J. Gen. Physiol.* **57**:593
31. Hanai, T., Haydon, D.A., Taylor, J. 1964. An investigation by electrical methods of lecithin in hydrocarbon films in aqueous solutions. *Proc. R. Soc. London A* **281**:377
32. Hanai, T., Haydon, D.A., Taylor, J. 1966. The influence of lipid composition and of some adsorbed proteins on the capacitance of black hydrocarbon membranes. *J. Theor. Biol.* **9**:422
33. Jost, W. 1960. Diffusion in Solids, Liquids and Gases. (2nd ed.) Academic Press, New York
34. Kaplan, J.H., Scorah, K., Fasold, H., Passow, H. 1976. Sidedness of the inhibitory action of disulfonic acids on chloride equilibrium exchange and net transport across the human erythrocyte membrane. *FEBS Lett.* **62(2)**:182
35. Knauf, P.A., Rothstein, A. 1971. Chemical modifications of membranes. I. Effects of sulfhydryl and amino reactive reagents on anion and cation permeability of the human red blood cell. *J. Gen. Physiol.* **58**:190
36. Lakshminarayanaiah, N., Murayama, K. 1975. Estimation of surface charges in some biological membranes. *J. Membrane Biol.* **23**:279
37. Lepke, S., Fasold, H., Pring, M., Passow, H. 1976. A study of the relationship between inhibition of anion exchange and binding to the red blood cell membrane of 4,4′-diisothiocyano-stilbene-2,2′-disulfonic acid (DIDS) and its dihydro derivative (H_2DIDS). *J. Membrane Biol.* **29**:147
38. Lepke, S., Passow, H. 1971. The permeability of the human red blood cell to sulfate ions. *J. Membrane Biol.* **6**:158
39. Lepke, S., Passow, H. 1973. Asymmetric inhibition by phorizin of sulfate movements across the red blood cell membrane. *Biochim. Biophys. Acta* **298**:529
40. Lessin, L. S. 1975. Red Cell Shape. M. Bessis, R. Need and J. Leblond, editors. p. 151. Springer Verlag, Heidelberg

41. Lieb, W.R., Stein, W.D. 1974*a*. Testing and characterizing the simple pore. *Biochim. Biophys. Acta* **373**:165
42. Lieb, W.R., Stein, W.D. 1974*b*. Testing and characterizing the simple carrier. *Biochim. Biophys. Acta* **373**:178
43. Mueller, T.J., Morrison, M. 1975. The transmembrane proteins in the plasma membrane of normal human erythrocytes. Evaluation employing lactperoxidase and protease. *Biochemistry* **14**:5512
44. Parsegian, A. 1969. Energy of an ion crossing a low dielectric membrane: Solution to four relevant electrostatic problems. *Nature (London)* **221**:844
45. Passow, H. 1969. Passive ion permeability of the erythrocyte membrane. *Prog. Biophys. Mol. Biol.* **19(2)**:423
46. Passow, H., Fasold, H., Zaki, L., Schuhmann, B., Lepke, S. 1975. Membrane proteins and anion exchange in human erythrocytes. *In:* Biomembranes: Structure and Function. Vol. 35. G. Gardos and I. Szasz, editors. p. 197. Hungarian Academy of Sciences, Budapest
47. Passow, H., Schnell, K.F. 1969. Chemical modifiers of passive ion permeability of the erythrocyte membrane. *Experientia* **25**:460
48. Poensgen, J., Passow, H. 1971. Action of 1-fluoro-2,4-dinitrobenzene on passive ion permeability of the human red blood cell. *J. Membrane Biol.* **6**:210
49. Obaid, A.L., Rega, A.F., Garrahan, P.J. 1972. The effect of maleic anhydride on the ionic permeability of red cells. *J. Membrane Biol.* **9**:385
50. Rothstein, A., Cabantchik, Z.I. 1974. Protein structures involved in the anion permeability of the red blood cell membrane. *In:* Comparative Biochemistry and Physiology of Transport. I. Bolis, K. Bloch, S.E. Luria, and F. Lynen, editors. p. 354. North-Holland, Amsterdam-London; American Elsevier, New York
51. Rothstein, A., Cabantchik, Z.I., Balshin, M., Juliano, R. 1975. Enhancement of anion permeability in lecithin vesicles by hydrophobic proteins extracted from red blood cell membranes. *Biochem. Biophys. Res. Commun.* **64(1)**:144
52. Rothstein, A., Takeshita, M., Knauf, P. 1972. Chemical modification of proteins involved in the permeability of the erythrocyte membrane to ions. *In:* Biomembranes. Vol. 3. Passive permeability of cell membranes. F. Kreuzer and J.F.G. Slegers, editors. p. 393. Plenum Press, New York-London
53. Schnell, K.F. 1972. On the mechanism of inhibition of the sulfate transfer across the human erythrocyte membrane. *Biochim. Biophys. Acta* **282**:265
54. Schnell, K.F. 1974. Untersuchungen zum Mechanismus des Sulfattransportes durch die Erythrozytenmembran. Habilitationsschrift, Universität Regensburg
55. Schnell, K.F., Gerhardt, S. 1973. The effect of the membrane potential on the anion exchange across the erythrocyte membrane. *Pfluegers Arch.* **343**:R60
56. Schnell, K.F., Gerhardt, S., Lepke, S., Passow, H. 1973. Asymmetric inhibition by phlorizin of halide movements across the red blood cell membrane. *Biochim. Biophys. Acta* **318**:474
57. Schnell, K.F., Gerhardt, S., Schöppe-Fredenburg, A. 1977. Kinetic characteristics of the sulfate self-exchange in human red blood cells and red blood cell ghosts. *J. Membrane Biol.* **30**:319
58. Singer, S.J., Nicholson, G.L. 1972. The fluid mosaic model of the structure of cell membranes. *Science* **175**:720
59. Stark, G., Ketterer, B., Benz, R., Läuger, P. 1971. The rate constants of valinomycin-mediated ion transport through thin lipid membranes. *Biophys. J.* **11**:981
60. Steck, T.L. 1974. The organization of the proteins in the human red blood cell membrane. *Biology* **62**:1

61. Steck, T.L., Ramos, B., Strapazon, E. 1976. Proteolytic dissection of band 3, the predominant transmembrane polypeptide of the human erythrocyte membrane. *Biochemistry* **15(5)**:1154
62. Sutherland, R.M., Rothstein, A., Weed, R.I. 1967. Erythrocyte membrane sulfhydryl groups and cation permeability. *J. Cell Physiol.* **69**:185
63. Szabo, G. 1972. Lipid bilayer membranes. *In:* Membrane Molecular Biology. C.F. Fox and A.D. Keith, editors. p. 146. Sinauer Associated, Stamford
64. Takashima, S., Schwan, H.D. 1965. Dielectric dispersion of crystalline powders of amino acids, peptides and proteins. *J. Phys. Chem.* **69**:4176
65. Toyoshima, Y., Thompson, T.E. 1975. Chloride flux in bilayer membranes: The electrically silent chloride flux in semispherical bilayers. *Biochemistry* **14(7)**:1518
66. Toyoshima, Y., Thompson, T.E. 1975. Chloride flux in bilayer membranes: Chloride permeability of aqueous dispensions of single-walled bilayer vesicles. *Biochemistry* **14(7)**:1525
67. Van Lamsweerde-Gallez, D., Meessen, A. 1975. The role of proteins in a dipole model for steady-state ionic transport through biological membranes. *J. Membrane Biol.* **23**:103
68. Wallach, D.F.H., Weidekamm, E. 1973. The microarchitecture of erythrocyte membranes. *In:* Erythrocytes, Thrombocytes, Leukocytes. E. Gerlach, K. Moser, E. Deutsch and W. Wilmans, editors. p. 2. Thieme-Verlag, Stuttgart
69. Wieth, J.O. 1970. Effect of some monovalent anions on chloride and sulfate permeability of human red blood cells. *J. Gen. Physiol.* **207**:581
70. Wieth, J.O. 1972. The selective ionic permeability of the red cell membrane. *In:* Oxygen Affinity of Hemoglobin and Red Cell Acid Base Status. M. Rørth and P. Astrup, editors. p. 265. Munksgaard, Copenhagen
71. Wieth, J.O., Dalmark, M., Gunn, R.B., Tosteson, D.C. 1973. The transfer of monovalent inorganic anions through the red cell membrane. *In:* Erythrocytes, Thrombocytes, Leukocytes. E. Gerlach, K. Moser, E. Deutsch and W. Wilmans, editors. p. 71. Thieme-Verlag, Stuttgart
72. Wieth, J.O., Funder, J., Gunn, R.B., Brahm, J. 1974. Passive transport pathways of chloride and urea through the red cell membrane. *In:* Comparative Biochemistry and Physiology of Transport. L. Bolis, K. Bloch, S.E. Luria and F. Lynen, editors. p. 317. North-Holland, Amsterdam-New York
73. Wood, P.G., Passow, H. 1973. Some remarks on the current concepts of the mechanism of anion permeability. *In:* Proceedings of symposium on drugs and transport. B.A. Callingham, editor. MacMillan, London
74. Zaki, L., Fasold, H., Schuhmann, B., Passow, H. 1975. Chemical modifications of membrane proteins in relation to inhibition of anion exchange in human red blood cells. *J. Cell. Physiol.* **86**:471
75. Zwolinsky, B.J., Eyring, H., Reese, C. 1949. Diffusion and membrane permeability. *J. Phys. Colloid Chem.* **53**:1426